Chem Soc Rev

REVIEW ARTICLE

View Article Online
View Journal | View Issue

Cite this: *Chem. Soc. Rev.*, 2014, 43, 2680

Colloidal silicon quantum dots: from preparation to the modification of self-assembled monolayers (SAMs) for bio-applications

Xiaoyu Cheng,[ab] Stuart B. Lowe,[ab] Peter J. Reece[c] and J. Justin Gooding*[ab]

Received 8th October 2013

DOI: 10.1039/c3cs60353a

www.rsc.org/csr

Concerns over possible toxicities of conventional metal-containing quantum dots have inspired growing research interests in colloidal silicon nanocrystals (SiNCs), or silicon quantum dots (SiQDs). This is related to their potential applications in a number of fields such as solar cells, optoelectronic devices and fluorescent bio-labelling agents. The past decade has seen significant progress in the understanding of fundamental physics and surface properties of silicon nanocrystals. Such understanding is based on the advances in the preparation and characterization of surface passivated colloidal silicon nanocrystals. In this *critical review*, we summarize recent advances in the methods of preparing high quality silicon nanocrystals and strategies for forming self-assembled monolayers (SAMs), with a focus on their bio-applications. We highlight some of the major challenges that remain, as well as lessons learnt when working with silicon nanocrystals (239 references).

1. Introduction

Semiconductor nanocrystals, or quantum dots (QDs), are attractive nano-materials because of their unique optoelectronic properties. They possess strong absorption, size-tunable photoluminescent (PL) emission, high quantum yield (QY) and high stability against photobleaching.[1] This is primarily due to the confinement of charge carriers within the small physical

[a] *School of Chemistry, The University of New South Wales, Sydney, NSW 2052, Australia. E-mail: Justin.gooding@unsw.edu.au; Fax: +61 2 9385 6141; Tel: +61 2 9385 5384*
[b] *Australian Centre for Nanomedicine, The University of New South Wales, Sydney, NSW 2052, Australia*
[c] *School of Physics, The University of New South Wales, Sydney, NSW 2052, Australia*

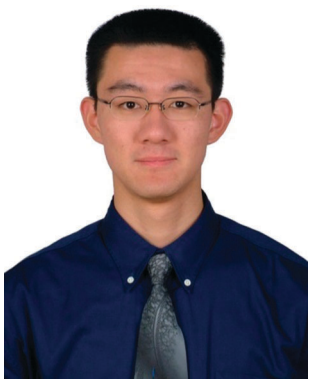

Xiaoyu Cheng

Xiaoyu Cheng graduated with BSc (Hons) with first class honours in Chemistry (2010) from the Australian National University. He worked with Prof. Gottfried Otting for his honours thesis on the development of new NMR spectroscopic methods for obtaining structural information of proteins. In 2011 he joined the group of Professor J. Justin Gooding for PhD studies at the University of New South Wales, where he has been ever since. His PhD work is concerned with the preparation, surface modification and bio-applications of colloidal silicon quantum dots. His research interests are in the material-biointerface and the development of functional nanomaterials.

Stuart B. Lowe

Stuart Lowe read for a Masters in Physics at the University of Oxford (2004–2008) before joining Prof. Molly Stevens' group at Imperial College London as a PhD student. During his PhD, he researched quantum dot-based platforms for analysis of enzyme activity, and was awarded his doctorate in 2012. Later that year, he joined the group of Prof. Gooding at UNSW as a postdoctoral research associate. His research interests include semiconductor nanoparticles, enzyme-responsive materials, and engineering cell-material interfaces.

dimensions defined by particle size, known as the quantum confinement effect.[2,3] The methods of preparation, surface properties and fundamental physics of compound semiconductor quantum dots have been well explored, including II–VI (*e.g.* CdX, X = Se, S, Te),[4–7] III–V (*e.g.* InP, InAs, GaAs),[8–10] and IV–VI (*e.g.* PbX, X = Se, S) quantum dots.[11–13] More recently, their applications in solar cells,[14–16] optoelectronic devices[17–19] and as fluorescent labelling agents[20–24] have been recognized and studied extensively, suggesting enormous potential for this class of material for a number of applications. However, one problem associated with traditional quantum dots is the use of heavy metal elements, such as cadmium which is known to be toxic to biological systems.[25–27] Safety issues therefore have hampered their development to some extent due to the current regulation on the use of heavy metals for commercial products,[27,28] which is particularly relevant with medically related products for *in vivo* purposes.[29–31]

Silicon is one of the most important materials on earth. It is abundant, relatively benign and widely used in microelectronic industry. Although an *indirect bandgap semiconductor* material and less interesting for light emitting device applications in the bulk form, the quantum confinement effect allows efficient fluorescence emission from silicon nanocrystals (SiNCs, silicon quantum dots or SiQDs),[32,33] with photoluminescence (PL) quantum yield (QY) up to 60–75%.[34,35] What we emphasize here are '*colloidal*' silicon quantum dots, or *freestanding* silicon nanocrystals,[36] as particles embedded in matrices such as thin films are another significant area of studies and beyond the scope of the current review. Two decades have passed since the first reports on silicon nanocrystals,[32,33] but challenges still remain in various aspects of working with this type of material. The first challenge is how to efficiently prepare high quality colloidal silicon nanocrystals in a feasible manner. This requires the particles to be made relatively simply with controlled size and optical properties. For this aim size tunable within 1–5 nm,[37] emission wavelength spanning from blue to near-IR (NIR) and QY above 10–15% are essential.[38,39] Another challenge is how to effectively modify the surface of silicon quantum dots, as freshly prepared silicon surface is prone to oxidation.[40,41] The impact of surface states is also significant for particles at this dimension,[42] due to the small exciton Bohr radius for silicon of merely 4.2 nm.[43] Both challenges, combined with difficulties in characterization, make SiNCs considerably more difficult to work with compared with conventional metal based quantum dots.

In spite of these challenges, the past two decades have seen rapid progress in methodologies in the preparation and surface modification of silicon quantum dots. Colloidal silicon nanocrystals can now be made with the desired optical properties and with reasonably complex surface architectures. For the sections below, we review critical steps of recent advancements in these areas. Section 2 gives a brief summary on the distinct physical features of quantum dots composed of silicon. In Sections 3 and 4, methods of preparation and strategies for surface modification are reviewed respectively. In Section 5, we focus on recent developments on applications of silicon quantum dots, highlighting fluorescent imaging studies in biological contexts.

2. Physical properties

Semiconductor quantum dots (QDs) are considered as artificial atoms: they exhibit discrete atomic-like density-of-states where the physical dimensions strongly affect the allowed energies of free electrons and holes.[5] Relaxation of free carriers across these discrete energy levels is a radiative process and yields the emission of a photon of equivalent energy.[44] The degree of confinement experienced by the electrons and holes, and hence emission wavelength, along with rates of radiative recombination, lifetimes, and quantum efficiency are largely governed by the dimensions of the dot, as well as the properties of the host material and surrounding barrier.[5,45] In an idealised scenario (*e.g.* a cubic dot with infinite potential barriers) the separation between energy states of electrons and holes can be described as the sum of the band gap energy of the host material, E_g,

Peter J. Reece

Peter Reece holds a BSc (Hons 1) in Medical Physics (1998) and a PhD in Physics (2005) from the University of New South Wales, where he developed novel silicon based photonic devices. From 2004–2007 he work on developing novel techniques of optical trapping and micromanipulation at the University of St Andrews, UK. In 2008 he was awarded a Vice Chancellor's Research Fellowship from the University of New South Wales and was appointed to a lectureship position in 2011. He currently works on various aspects of Nanophotonics, Biophotonics and Optoelectronics.

J. Justin Gooding

Scientia Professor Justin Gooding graduated with a BSc (Hons) from Melbourne University and completed a DPhil from the University of Oxford and postdoctoral training at the Institute of Biotechnology in Cambridge University. He returned to Australia in 1997 as a Research Fellow at the University of New South Wales and became a full professor in 2006. He is currently an ARC Professorial Fellow and a co-director of the Australian Centre for NanoMedicine. He leads a research team of 30 people interested in surface modification and nanotechnology for biosensors, biomaterials, electron transfer and medical applications.

and energy contributions for each of the confined dimensions (x, y, z) for the conduction and valence bands,[46] as well as a small contribution from exciton binding (not included):[47]

$$\Delta E = E_g + \sum_{i=x,y,z} \frac{\hbar^2 \pi^2 n_i^2}{2d_i^2}\left(\frac{1}{m_e} + \frac{1}{m_h}\right)$$

Here d_i is the size of the QD in the ith dimension, n is the quantum number, and m_e and m_h are the effective masses of the conduction band electrons and valence band holes, respectively. For large nanocrystals the confinement energies are negligible, however when the dimensions become comparable to the exciton Bohr radius of the host material the confinement energies become significant. These size-tuneable alterations of electronic states, and thus optical features of the particle, make QDs a distinct class of fluorophores.[48] In practice there are many physical factors that complicate the expected behaviour of electronic states and optical properties in QDs; they include finite potential barriers, band-offsets,[49] surface mediated effects,[50] band-structure related effects (degeneracy, critical points),[51] dark states, *etc.*[52,53] These must all be considered in understanding the details of the observed behaviour of the light emission process in QDs.

The physical properties of quantum confined semiconductor heterostructures have been investigated extensively in compound materials systems, such as III–V and II–VI QDs. Precise physical deposition methods, such as molecular beam epitaxy, have allowed the growth defect-free islands of low energy band gap material (*e.g.* InAs) inside a wider band gap host (*e.g.* GaAs).[54,55] The host material acts as a potential barrier that confines conduction band electrons and valence band holes within the dots and also acts to passivate the structures against surface related effects.[54] III–V QDs, whilst having no utility in biolabelling applications, have provided a great deal of fundamental information on the nature of quantum confinement in solid state systems and have significant applications in technological areas of optoelectronics and quantum information.[56,57] Chemically synthesised II–VI compound QDs are a colloidal analogue of conventional III–V QDs: they have a core–shell structure, where the wider band-gap semiconductor (*e.g.* ZnS) provides a confining potential for the smaller band gap (*i.e.* CdSe, CdTe *etc.*) core region.[4,8] In addition, II–VI QDs have an organic capping layer that stabilises the colloid in solution and can be used for further functionalization for specific applications.[45] Synthesis is based on a mature process where size dispersity and optical properties can be controlled with excellent precision.[45]

2.1 Comparison between quantum dots and organic dyes

In general, essential physical features for fluorophores include the absorption and emission profiles, spectral position, blinking, full width at half maximum (FWHM), brightness, fluorescence lifetime, quantum yield and the Stokes shift[1] (Table 1).

The most frequently used fluorophores today are organic dyes, which are widely used in various biological and biochemical assays.[58] Although there are several reviews in literature comparing the properties of QDs and organic dyes,[1,45] emphasis is still given here due to the importance of the topic. In comparison to conventional organic dyes, fluorescent QDs are endowed with several attractive properties (Table 2).

One critical property of QDs as fluorophores is related to the broad absorption profile accompanied by a narrow, wavelength-tunable emission peak.[59] The broad absorption spectrum of QDs allows efficient excitation, which is desirable when the number of available photons for excitation is limited. QDs also usually possess much larger molar absorption coefficients (up to 100 000 000 M^{-1} cm^{-1})[59,60] at the excitation peak wavelength compared with organic fluorophores (up to 250 000 M^{-1} cm^{-1}).[61,62] In addition, the emission bands of organic dyes are often unsymmetrical,[63] whose red 'tail' is not seen in the emission profiles of QDs. Position of the emission peak in QDs is also tunable by varying size of the particle,[64] which is not possible for organic dyes. This has made multicolour imaging using QDs by the same incidence light source possible, whereas only limited wavelength choices are available for dye staining.[64]

A second advantage of QDs over organic dyes is its high quantum yield, especially in the near infrared (NIR) region. For organic dyes, QY is usually high in the visible region, but below 20% in the NIR region.[63] In the case of QDs, quantum yield can reach up to 60% to 80% in both the visible and NIR region depending on the core materials.[65–68] A third major difference is the significantly longer fluorescent lifetime of QDs compared with organic dyes. Fluorescent lifetimes for most organic dyes are less than 5 ns in the visible region and sometimes less than 1 ns in the NIR region,[69] causing difficulties for temporal discrimination between fluorescence interference and scattering from the excitation wave.[69] In contrast, most QDs have fluorescent lifetimes to 10 ns, sometimes reaching several tens of ns even μs for red emitting silicon quantum dots, allowing sensitive separation between signals from auto-fluorescence and scattered excitation light by time-gated imaging techniques.[70]

Due to the use of heavy metal elements in conventional QDs, they are considered by many to be not suitable for large scale bio-applications, particularly for *in vivo* applications.

Table 1 Glossary of terms used

Absorption/emission band	A range of wavelengths in the spectrum where a particular photon can be absorbed/emitted from a substance
Blinking	Excited fluorophores emit light for limited time, disrupted by periods when no emission occurs
Full width at half maximum	Width of the emission peak at which half of its intensity is observed
Brightness	Product of the molar extinction coefficient and quantum yield, measured at the excitation wavelength
Fluorescence life time	Time needed for intensity of fluorescence to decay to 1/e of its maximum value
Quantum yield	Efficiency of the fluorescence process, defined as ratio of the number of photons emitted to the number of photons absorbed
Stokes shift	Difference of wavelength between the absorption/emission peaks

Table 2 Comparison between QDs and organic dyes

Property	Organic dyes	QDs
Absorption profile	Narrow, discrete bands, FWHM ranges from 35 nm to 80–100 nm	Broad, unsymmetrical profile, increase steadily towards UV region
Emission profile	Asymmetric, FWHM 35 nm to 70–100 nm	Gaussian profile, FWHM, 30–90 nm
Stokes shift	Usually less than 50 nm	Usually less than 100 nm
Quantum yield	0.5–1 (visible), 0.05–0.2 (NIR)	0.1–0.8 (visible), 0.2–0.7 (NIR)
Fluorescent lifetimes	1–5 ns	5–100 ns, up to μs for some red SiQD
Photochemical stability	Sufficient in the visible region, but can be insufficient for NIR dyes	High, sufficient in both visible and NIR regions
Multiple colours	Possible by varying molecular structure	Adjustable by varying size

Therefore, in this review we concentrate on the bio-applications of SiQDs. However, SiQDs possess distinct physical properties compared with conventional QDs, as we will explain in Section 2.2.

2.2 Important physical properties of silicon quantum dots

Unlike conventional core–shell QDs, silicon quantum dots (SiQDs) are usually prepared with hydrogen, halogen or oxide terminated surface. Due to the lack of a lattice-matched semiconductor barrier layer, surface properties are of particular significance in defining the photophysics of SiQDs. The different potential barriers affect the photoluminescence (PL) properties, including wavelength of the emission peak, quantum yield (QY), appearance of subsidiary peaks and fluorescence lifetime (τ).[71] In terms of the emission profile, absence of a semiconductor shell reduces the degree of exciton confinement in the core and broadens the emission peak. In practice, SiQDs prepared *via* colloidal solution methods were predominantly blue-green in colour, whilst red dots with broad emission can only be prepared *via* high temperature or etching related methods thus far (Fig. 1). In addition, there have been attempts to red-shift the emission profile of blue emitting SiQDs by doping with substituent atoms.[72,73] Noticeably, because of the small size of SiQDs, any dopant atoms incorporated are present at concentrations that would be considered 'heavy doping' and furthermore SiQDs may be doped stochastically, resulting in sub-populations of doped and undoped SiQDs.[74,75] In terms of QY, the existence of imperfections and defects at the surface of SiQDs can affect QY by providing alternative decay pathways. In most cases, additional decay pathways associated with surface capping ligands may become the dominant factor of causing reduction in QY,[76] and can lead to the appearance of subsidiary blue/green emission peaks *via* surface-associated recombination.[42,71,77] Interestingly, certain electron donating, nitrogen containing species at particle surface strongly increase QY of SiQDs, as was shown in a recent study.[35] It was suggested that surface capping of SiQDs with organic ligands has led to distortion of electronic structure, which was evidenced by scanning tunnelling microscopy.[77] Oxidation of larger SiQDs has been shown to affect the crystallinity and core diameter of the Si nanocrystals, reducing the QY and blue-shifting the wavelength of emission peak.[34,78] However, modification of the SiQD surface with an organic monolayer can prevent the long-term oxidation, providing more stable PL properties.[79] In terms of lifetime, short fluorescence lifetime (order of ns) in SiQDs is often associated with core-related recombination.[80] Much longer lifetime (order of μs) in SiQDs has been observed, which was suggested to be due to the existence of ultrafast trapping of excited carriers in surface states, preventing core recombination.[81]

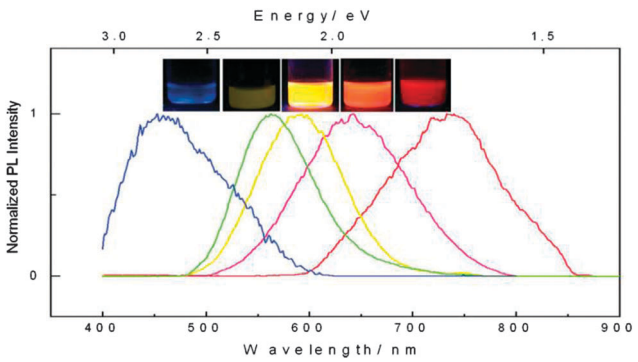

Fig. 1 Photoluminescence spectra and corresponding fluorescence colors of SiQDs produced by controlled etching conditions. Reprinted with permission from Gupta *et al.*[78] Copyright 2009 Wiley-VCH.

Conventional QDs are usually made from semiconductor materials with a direct bandgap. The radiative transition pathway in SiQDs is different in character from that of conventional QDs because bulk silicon is an indirect bandgap semiconductor. In terms of the bio-applications of SiQDs, a detailed discussion of the SiQD electronic structure is beyond the scope of this review. However, it is worth mentioning that the exciton recombination rate is higher than that observed in bulk silicon because quantum confinement increases the uncertainty in k vector, meaning that previously unfavoured transitions are accessible. Veinot *et al.* suggest that,[36] as well as confinement, surface effects may also be responsible for the observed rate of dipole-mediated radiative decay. Because it can be difficult to separate surface and confinement effects in free-standing colloidal nanocrystals, some work has been done to study this transition in systems where the SiQDs are embedded in a matrix.[82]

Similarly to conventional quantum dots, many preparations of SiQDs display decreased PL when transferred into aqueous solution. But the PL could be maintained by encapsulating SiQDs in phospholipid micelles.[83] The origin of PL quenching of SiQDs upon transfer to aqueous media has been suggested to originate from the formation of non-radiative oxide-related states during surface treatments designed to render the SiQDs water soluble.[84] Despite this, water-soluble SiQDs have been

shown not to suffer from photobleaching under conditions which photobleached conventional organic dyes.[80] Blinking of PL fluorescence is a commonly-observed phenomenon in fluorescent molecules including SiQDs.[85] Galland *et al.* have suggested that the origin of blinking in semiconductor QDs is due to a combination of multiple effects; (i) non-radiative recombination caused by excess charges; and (ii) charge fluctuations in electron-accepting surface sites.[86]

Although SiQDs possess many of the desired physical properties for bio-applications, in order for them to be effective in practical contexts, the effect of preparation method and surface functionalization must be considered with respect to both photophysical features and biological interactions. These aspects will be reviewed in the following sections.

3. Methods of preparation

Numerous methods have been developed for preparing colloidal silicon quantum dots (SiQDs). Similar to the methods of preparing many types of nanostructures, these methods can be roughly classified as either 'top-down' approaches, *i.e.* breaking down large pieces of silicon to smaller nanoscale pieces, or 'bottom-up' approaches that primarily rely on self-assembly processes using molecular silicon precursor species. Due to the interdisciplinary nature of some methods, a third class of methods can be classified based on the involvement of both 'top-down' and 'bottom-up' components. Here, developments of methods for preparing colloidal SiQDs are summarized.

3.1 The top-down approach

3.1.1 Etching of bulk silicon. One of the most popular methods for preparing colloidal silicon nanocrystals (SiNCs) is *via* etching of bulk silicon. Sailor *et al.* first demonstrated this process with a mixture of HF and H_2O_2 to electrochemically etch porous silicon with the aid of ultrasound, and created a 'luminescent colloidal suspension'.[239] The suspension was found to contain nanometer-sized silicon particles with crystalline structures.[239] Due to its relative simplicity, this approach rapidly gained attention, and has been widely used ever since.[88,89] For instance, it was recently shown that etching of silicon powder with the assistance of ultrasound and a combination of HNO_3–HF produced silicon nanoparticles with controlled wavelength of emission.[89]

In addition, Kang *et al.* developed a variant of the etching method where the colour was tuneable from blue to red as determined by the size of the particles (Fig. 2).[90] In this design, a graphite rod was used as the anode and silicon wafer as the cathode. One of the keys to this method was polyoxometalates where their unique ability to be an electron donor and acceptor simultaneously was exploited.[90] Altering the current density was used to adjust the size of particles upon HF/H_2O_2 etching, producing shape and size controlled hydrogen terminated silicon nanoparticles with size ranging from 1–4 nm and emission peak between 450–700 nm.[90] The etching mixture was further modified to provide control over the oxidizing

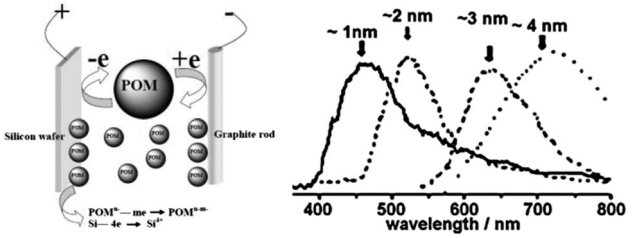

Fig. 2 Polyoxometalates assisted electrochemical etching process of preparing colloidal SiNCs. Reprinted with permission from Kang *et al.*[90] Copyright 2007 American Chemical Society.

environment using a mixture of H_2O_2 and ethanol,[91] such that the larger particles (3 nm) were partially oxidized to yield small crystalline silicon cores in an oxide shell. As a result, oxide coated silicon nanocrystals of 1–3 nm with a wide spectrum of colours were obtained.[91] Although it has been reported elsewhere that simple sonication of porous silicon without etching sometimes yield photoluminescent particles,[92–94] it is important to realize that these micrometre sized particles contain domains of silicon nanoparticles in them, rather than colloidal silicon quantum dots which is the focus of this review.

3.1.2 Breaking down silicon rich oxides. A second class of the top-down approaches is based on the breakdown of silicon rich oxides containing silicon nanocrystals (Fig. 3). Usually, silicon nanocrystals are annealed within a SiO_x matrix, which are formed from precursors such as silicon sub-oxides (*i.e.* Si_mO_n).[96,97] The strategy was first reported by Liu *et al.* where colloidal silicon nanocrystals were obtained by etching away the oxide layer from thermally annealed, amorphous, commercial SiO_x powder.[98,99] It was confirmed by TEM studies that size of the final nanocrystals ranged from 2 nm to 16 nm depending on etching conditions, and lattice fringes were visible through HR-TEM observations. Comparatively, Hessel *et al.* utilizes thermal decomposition of hydrogen silsesquioxane to produce bulk amount of silicon rich oxides as thin films under high temperature.[95,100–102] This is followed by controlled HF etching to give colloidal, hydride terminated silicon quantum dots with emission wavelength tuneable in the entire visible spectrum.[95,100–102] There have been other attempts of using sol–gel polymer precursors for preparing silicon quantum dots, however these methods have been reviewed in detail elsewhere,[103] therefore are not included in the current review.

3.1.3 Advantages and drawbacks. To summarize, a major advantage for most top-down methods is the good compatibility with studies of flat or porous silicon structures in terms of procedures used and techniques required. Also, most top-down methods showed good control of emission wavelength that cannot be easily achieved by other methods. However, the HF frequently used is often in much higher concentration than needed for preparing other silicon surfaces, with 48% HF applied in some cases.[38,83,89,104] The relative harsh conditions required for the heat treatment of silicon rich oxides is also critical for successful generation of nanoparticles within them before the etching step, a process not easily approachable by non-experts.[95,102,105] Both issues have hampered these methods

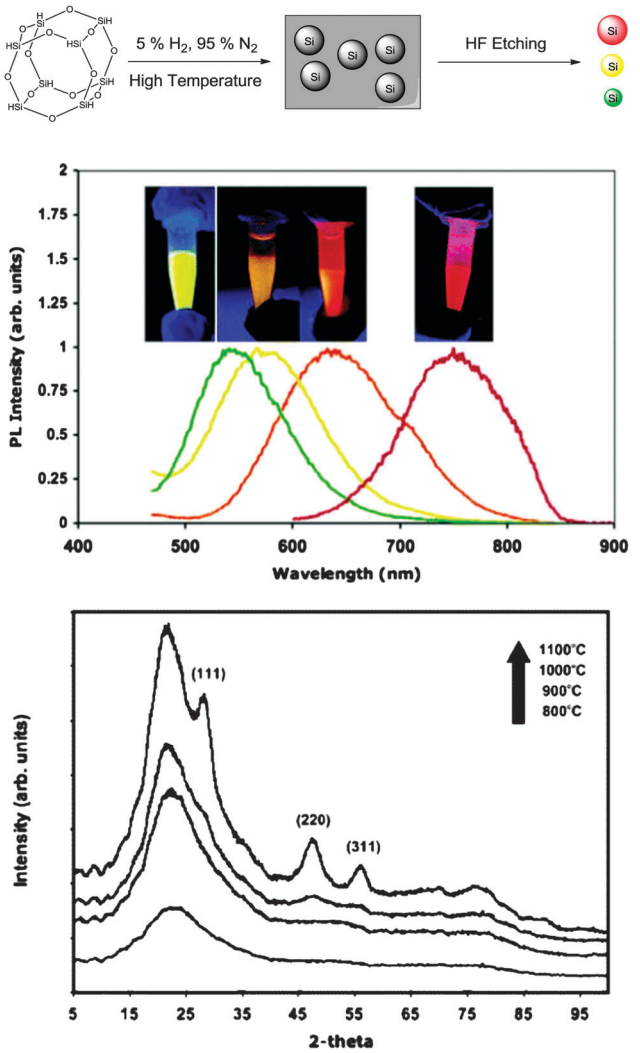

Fig. 3 Preparation of colloidal silicon nanocrystals by breaking down silicon rich oxides containing nanoparticles within them. Reprinted with permission from Hessel *et al.*[95] Copyright 2006 American Chemical Society.

from progressing towards large scaled production or wide applicability, due to the high safety risk involved and specific techniques required for the processes.

3.2 The bottom-up approach

The alternative to the top-down routes mentioned above to prepare colloidal silicon nanocrystals is *via* assembly of small molecular precursors. That is, *via* a bottom-up approach.

3.2.1 Solution based precursor reduction. One class of bottom-up procedures uses reducing agents in the presence of silane precursors in solution. The method was initially demonstrated by Heath in 1992, who showed that mixing $SiCl_4$ and octyltrichlorosilane under high temperature and pressure produced polydispersed silicon nanoparticles.[108] Due to the relative simplicity of the approach, numerous variants of this method have been established. Examples include the use of sodium naphthalenide ($NaC_{10}H_8$) as the reducing agent and $SiCl_4$ in glyme solution,[109] or sodium (Na) as the reducing agent and tetraethyl orthosilicate (TEOS) in a bomb reactor.[110] Both methods yielded silicon quantum dots with a size of several nanometers with visible blue luminescence.[109] However, one disadvantage was the poor control of particle size, with particle diameter usually ranging over tens of nanometers within a single batch.[109] To assist with reducing particle size distribution, it was reported that addition of surfactant molecules to the reaction mixture, to create inverse micelle environments, provided a greater ability to control the size. This remarkable improvement was first demonstrated by Wilcoxon *et al.*,[111] and more recently advanced by Tilley *et al.*[80,106] In a typical experiment, tetraoctylammonium bromide (TOAB), a phase transfer agent and surfactant, stabilized the halogenated silane precursors in toluene, allowing relatively homogeneous precipitation of silicon nanocrystals within the inverse micelle upon addition of lithium aluminum hydride.[80,106] This method generated hydrogen terminated silicon nanocrystals with narrow size distribution, *i.e.* FWHM of emission peak below 80 nm and size of 2–3 nm within one batch.[80,107,112,113] Generally this method produces only blue luminescent colloidal silicon nanocrystals. To date it is still difficult to obtain a full range of colours with the reduction method. Furthermore, separating the surfactant from the reaction mixture is not a trivial task,[107] albeit not impossible with size-exclusion chromatography.[113] To avoid the tedious purification steps, it was recently shown that silanes with carbon rich side chains can function as a replacement for the surfactant TOAB.[114] This led to very facile methods of preparing silicon nanocrystals with essentially no purification processes,[114] while at the same time giving easily accessible surface moieties for further functionalization.[115] Again however the quantum dots obtained are only blue in colour (Fig. 4).

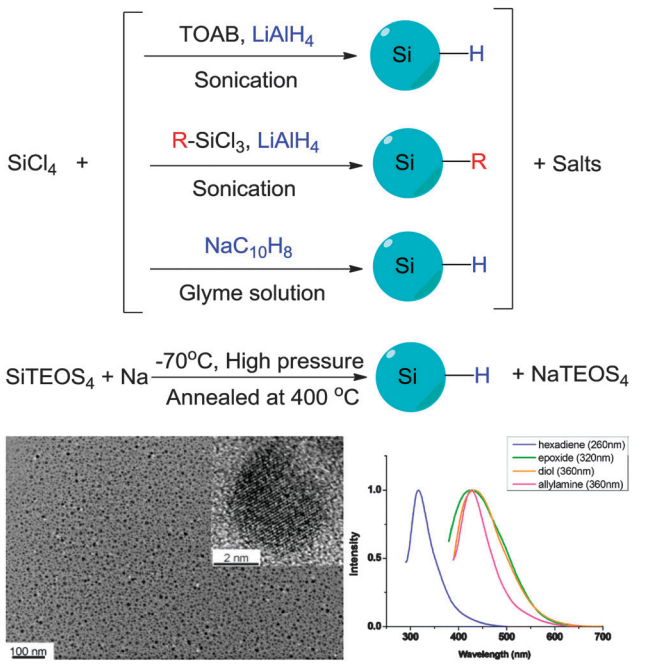

Fig. 4 Preparation of colloidal silicon nanocrystals *via* solution based precursor reduction. HR-Tem images confirm crystal structure of the particles obtained, with fluorescence in the UV-blue region under UV excitation. Reprinted with permission from Tilley *et al.*[106,107] Copyright 2010 American Chemical Society.

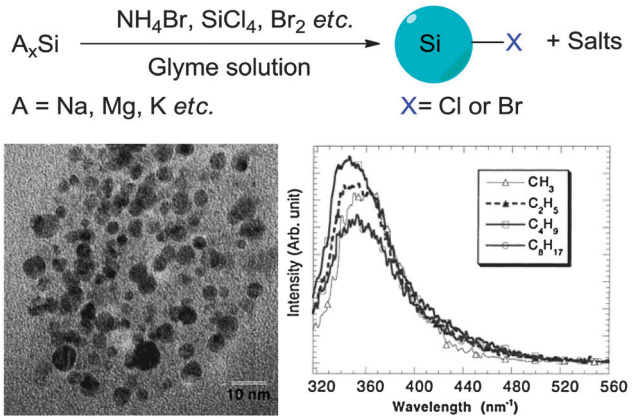

Fig. 5 Zintl salts based synthetic methods of preparing SiNCs. Reprinted with permission from Yang *et al.*[116] Copyright 1999 American Chemical Society.

3.2.2 Development of Zintl salt based approaches. A second class of reaction for the bottom-up preparation of silicon nanocrystals utilizes silicon Zintl salts (*i.e.* ASi_x, A = Na, K, Mg *etc.*). Typically with this class of method a silicon Zintl salt is reacted with silicon halides, or bromine gas. For instance, Kauzlarich *et al.* prepared silicon nanocrystals *via* reactions between potassium silicide (KSi) and $SiCl_4$ in boiling glyme or diglyme solution[109,116–120] (Fig. 5). Relevant FT-IR analysis confirmed that the prepared nanoparticles were initially halogen species coated but further functionalized with methoxy groups during the work up step in which methanol was used for washing.[119] A comparable method was developed by using sodium silicide (NaSi) and ammonium bromide (NH_4Br). The method also gave blue luminescent silicon nanocrystals with average size of ~4–5 nm but with reasonably large amounts of tens of milligrams per batch.[121] Comparative results were obtained for reaction between magnesium silicide ($MgSi_2$) and bromine gas (Br_2),[122] as well as between NaSi and $SiCl_4$ in boiling glyme solution.[117]

3.2.3 Advantages and drawbacks. Recognized features of the bottom-up methods are: First, they are more often based on colloidal 'chemical', rather than 'physical' means, and hence more readily performed in solution. Second, usually common reagents and equipment that are compatible with conventional bench top chemistry are used. This also made surface chemistry of the particles more easily accessible, which is essential for both preparation and characterization. Finally, it is not uncommon with these methods to yield good amount of products with reasonable quality, an important factor to consider when scaling up the production for application contexts.

In contrast, an obvious problem with solution bottom-up methods is the lack of full spectrum of colour, with only blue-green colour accessible to date. Regardless the fact that red emitting dots can be made with laser pyrolysis and non-thermal plasma synthesis, variation of particle emission wavelength with the bottom-up approach has this far only been achieved by further etching the particles with concentrated HF, which is essentially a top-down approach. Also, although there are recent reports demonstrating that very high QY SiQDs can be synthesized by this class of method,[35] particles prepared using bottom up approaches usually exhibited much lower quantum yield compared with top-down approaches, with quantum yield rarely exceeding 15%.

3.3 Precursor decomposition and re-assembly

A third class of methods typically involves the decomposition precursor species containing silicon heteroatoms and re-assembly processes to form SiQDs. Methods belonging to this class are distinct to previously discussed methods due to the multiple processes needed, which usually involve both the top-down and bottom-up steps.

3.3.1 Preparation in supercritical fluids. One method to decompose precursor species and re-assemble residues to nanoparticles is pioneered by Korgel *et al.*, who showed successful synthesis of silicon nanocrystals in supercritical fluids.[101,123,124] In a typical set-up, alkoxy-coated crystalline silicon were prepared by allowing the degradation of diphenylsilane under high pressure and high temperature.[123] The reaction was performed in a mixture containing octanol and hexane, which was heated to 500 °C and applied with pressure of 345 bar.[123] This approach generated silicon nanocrystals with comparatively good yield of 0.5–1.5% (several tens of milligrams) per batch and quantum yield of up to 5%, arguably due to good surface passivation of the octanol layer.[123,124] In a recent report by He *et al.*, it was shown that thermolysis process could be achieved by microwave heating, with silicon nanowires and glutaric acid as the precursor species.[125] The prepared silicon quantum dots were measured by HR-TEM to have an average size of ~3.1 nm, had good water dispersity, high pH/temperature stability, and excellent biocompatibility.[125]

3.3.2 Laser pyrolysis. Laser pyrolysis has emerged as a powerful tool for generating freestanding silicon nanocrystals. This procedure was first demonstrated by Cannon *et al.*, using a set-up that involved the focus of a high power laser beam on a stream of silane gas.[87,126] Laser irradiation induced high temperature of up to 1000 °C close to the point where the beam intersected with the gas, allowing formation of silicon nanocrystals in this area.[87,126] In spite of the initial success of this method, strong photoluminescence was detected only in limited cases in subsequent studies, when pyrolysis products were etched with HF, and yield of final product was usually very low.[127–131] Li *et al.* recently advanced this method by first preparing silicon nanoclusters of up to 50 nm, achieved *via* CO_2 laser induced pyrolysis of SiH_4 gas in an aerosol reactor.[38] This treatment was followed by controlled etching using a mixture containing highly concentrated hydrofluoric acid (HF) (48%) and nitric acid (HNO_3).[38] It was reported that silicon quantum dots with colour tunable in the entire visible spectrum can be prepared in a rate of ~20–200 mg per hour with quantum yield lying in the range between 2–15%.[38,132] Higher QYs (up to 39%) have been achieved in more recent work.[133]

3.3.3 Plasma synthesis. Although more often used for preparing nanoparticles embedded within thin films, it has been established that non-thermal plasma can also be used for

the synthesis of freestanding silicon nanoparticles. In principle, hot electrons in the plasma result in dissociation of precursor molecules, such as SiH_4.[134] This process initiates the nucleation step, and subsequent anion-molecule interactions allow the growth of particle core.[134] As particle density increases and ion density decreases, eventually the growth rate slows down. Since the unsaturated Si_nH_m clusters are positively charged, electrons readily attach to them, causing the clusters to be electrostatically confined in the plasma.[134] This is a critical difference to other pyrolysis methods (*i.e.* thermal or laser) in which there is essentially no mechanism to stop particle growth. One of the successful examples of synthesizing freestanding silicon nanoparticles with this method was shown by Viera *et al.*, with measured particle sizes of ~10 nm.[135,136] Kortshagen *et al.* and Oda *et al.* also succeeded in demonstrating several plasma processes, producing silicon nanoparticles with sizes ranging from a few to several tens of nanometers.[34,39,137–145] The design shown by Kortshagen *et al.* was able to produce silicon nanocrystals with quantum yield of up to 60%.[34] Variants of the methods were reported by different groups, including the use of microwave discharger that operated at low,[146] or atmospheric pressure,[147] respectively.

3.3.4 Advantages and drawbacks. A clear advantage of methods belonging to this class is the wide choices of colour of particles obtained. Unlike most of the bottom-up, solution based methods, where only blue-green colours are accessible, red to orange fluorescence can be obtained using majority of procedures belonging to this class. This is particularly favoured for bio-applications due to the existence of tissue window which lies in the range between ~650 nm to ~1000 nm. Another advantage is the high quantum yield from many procedures. QY for some of the non-thermal plasma methods can reach up to 60–70%, which cannot be easily achieved by most solution methods. A third advantage of methods belonging to this class is that for certain gas-phase, plasma based methods, production of silicon 'nano-inks' at industrial scale has become achievable, nevertheless direct evidence of whether these nanoparticles are 'quantum dots' is still unavailable.[134,141]

One disadvantage of methods belonging to this class is the use of specialized equipment. Temperature required for decomposing the precursor species is often very high, despite in some non-thermal plasma processes the actual operating temperature is close to room temperature. Highly toxic chemicals and procedures (*i.e.* HF etching) are often used, which requires strict control of every step in the preparation process due to the safety concerns.

4. Surface modifications

In contrast to the well-established methods of surface modification for II–IV semiconductor quantum dots,[148] very different procedures are used for forming self-assembled monolayers (SAMs) on colloidal silicon quantum dots. Despite the use of silica shell for surface modification in some cases,[149–151] probably the most common approach for introducing surface moieties to colloidal II–IV quantum dots is still *via* ligand exchange.[152] Ligand exchange principle relies on replacing surfactant molecules with ligands with strong affinity with surface of quantum dots, using thiols,[153–156] polymers,[157–159] or certain inorganic ligands.[160] However, comparable surface modification techniques for SiNCs typically require the formation of robust covalent linkages, usually between surface silicon atoms and carbon, nitrogen or oxygen species[161] (Table 3). This is particularly important in preventing the oxidation of pristine silicon surfaces. Despite increasing interest in the surface passivation of SiQDs, complete characterization of the surface remains a challenge. The challenge is particularly evident when considering the incomplete coverage of organic monolayers on flat and porous silicon surfaces.[161–166] In this section, we discuss recent methodological advances in surface modification of colloidal silicon quantum dots.

4.1 Wet-chemical based modification strategies

4.1.1 Formation of SAMs by hydrosilylation. Hydrosilylation is arguably the most important method of surface modification for colloidal silicon nanocrystals (SiNCs) (Fig. 6). Performing hydrosilylation reaction on SiNCs is in a way similar to the widely used approach for assembling organic monolayers on bulk silicon surfaces, as first demonstrated by Linford and Chidsey.[40,41] Fundamentally speaking, hydrosilylation requires the preparation of hydrogen terminated colloidal SiNCs.

Table 3 Schematic of strategies of surface modification of colloidal silicon quantum dots by forming covalent linkages

Surface of SiQDs	Surface modification strategies	Example of distal moieties
Hydride terminated surface	Hydrosilylation	Alkane Alkene NH_2 COOH
Halogen terminated surface	Nucleophilic Substitution	Hydrogen Alkane –OH

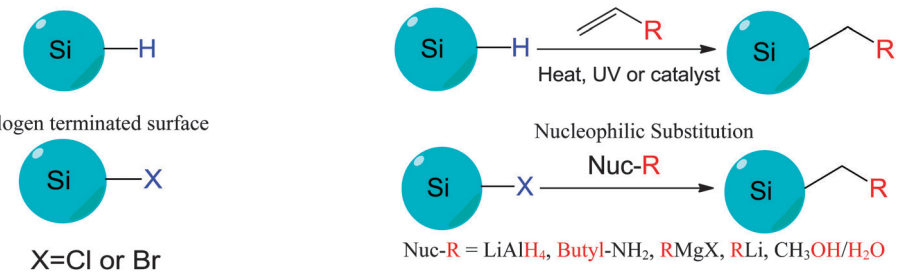

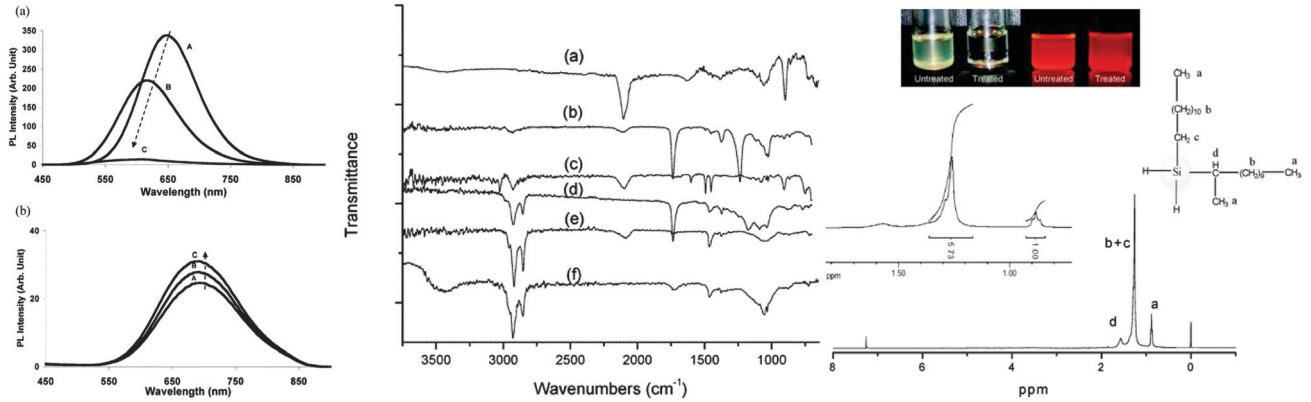

Fig. 6 Attachment of different surface moieties to SiNCs *via* hydrosilylation. The reaction is initiated by photo-, thermal or catalytical treatment. Left: (a) unmodified silicon quantum dots showed instable photoluminescence. (A) immediate after preparation, (B) after 1 day, (C) after 12 days in toluene. (b) Grafted particles with improved PL stability. (A) immediately after preparation, (B) after 35 days, (C) after 60 days in toluene. Middle: FT-IR spectra of silicon quantum dots with a range of surface groups (a) hydrogen, (b) vinyl acetate, (c) styrene, (d) ethyl undecylenate, (e) 1-dodecene and (f) undecanol. Right: modified silicon quantum dots have improved dispersity in solvents and strong fluorescence (top). The surface groups were characterized by ^{1}H-NMR spectroscopy (bottom). Reprinted with permission from Li *et al.* and Hua *et al.*[38,104] Copyright 2004 & 2005 American Chemical Society.

This step can be achieved by solution based reduction,[107–109] use of silicon Zintl salts,[117–120] etching,[38,84,91,104,167] or the use of non-thermal plasma,[34,39,141,142,168] as described in Section 3. The prepared hydrogen-terminated silicon nanoparticles possesses a distinct Si–H peak at $\sim$2100 cm^{-1} by FT-IR measurements.[38,39,104,118,119,141,169] Notice this absorption band is not necessarily shown on all reports. For example, direct evidence for this bond is still absent with some solution reduction based methods, regardless of strong indication of Si–H presence according to subsequent chemistries of successful grafting of surface molecules.[80,106,107,112,113,170] Interestingly, the Si–H bond on silicon quantum dots exhibits subtle differences compared with its bulk counterparts. For instance, the HF etching rate on silicon nanocrystals was shown to be much slower than that on bulk silicon, with only several nanometres per minute on particles *versus* micrometres per minute on bulk.[38,104,171] It was argued that a likely cause for the slow rate is the presence of fluorinated ions on the curved surface.[38,172] Furthermore, it was reported that HF alone often could not completely remove all oxides,[38] but the addition of ethanol and HNO_3 to the etching mixture greatly assisted the production of oxide free particle surface.[105,172]

The Si–H bonds on nanocrystals then readily react with alkene or alkyne moieties to form robust Si–C bonds on silicon nanocrystals under thermal, photochemical, or in rarer cases catalytical treatment (Fig. 1).[170] It was shown that both UV and near-UV irradiation allowed the attachment of alkenes on SiNCs' surface,[84,132,173] but the reaction rate was slower on larger particles using near-UV light of 365 nm.[84,173] Thermal methods have been equally successful with the hydrosilylation processes, with heating at 140 °C for 20 hours shown to attach alkenes on hydrogen terminated silicon quantum dots.[103] In addition, common catalyst for hydrosilylation reaction, such as chloroplatinic acid (H_2PtCl_6) was used to initiate the reaction,[107] though at a rate slower than thermal or photochemical activation.[170] In a recent report by Korgel *et al.*, it was shown that the process could occur even at room temperature with certain biofunctional alkenes, arguably because of the carboxylic acid facilitated nucleophilic attack on the curved surface.[174] Due to the wide choices of the distal moieties of the surface molecules, it has been demonstrated that hydrosilylation allowed direct coupling of various polar (*i.e.* –NH2, –COOH, $-SO_3^{2-}$) or non-polar (*i.e.* alkyl, alkenyl) moieties to the surface of silicon nanocrystals.[115,175–177]

Understanding the details of the mechanism of hydrosilylation is still the focus of intense studies and debates on bulk silicon surfaces, and much less work has been done with silicon quantum dots than bulk silicon. However, increasing evidence suggested that hydrosilylation on silicon nanocrystals happened in a comparable manner to flat or porous silicon[84,167,173] (Fig. 7). Recently, it was depicted that hydrosilylation occurred *via* either a free radical or exciton mediated mechanism on particle surface.[84,173] In the free radical initiated process (Fig. 7a), a hydride homolysis step due to thermal or photochemical treatment leads to the generation of free radicals, which allow the addition of alkene moiety in a chain of propagation process. In the exciton activated mechanism (Fig. 7b), no radical is generated, but photochemical generated excitions allow directly addition of nearby alkene moieties with the Si–H bonds, a comparable process to what happens on bulk silicon (Fig. 7c).[84,173]

4.1.2 Modification of halogen coated silicon nanocrystals. A second route of surface modification for silicon nanocrystals is based on reactions of the surface Si–Cl or Si–Br moieties. Silicon quantum dots with chloride surface are usually prepared by the reaction of silicon Zintl salt (ASi: A = Na, Mg, K) and $SiCl_4$, as discussed in Section 3.2.2.[109,116,118,119] The strong electrophilic reactivity and versatility of the Si–Cl bond were utilized for the attachment of a range of surface molecules. For example, rinsing chloride coated particles with methanol/water resulted in hydrophobic methoxy surfaces; common nucleophilic reagents such as alkyl lithium and Grignard reagents allow alkyl attachments;[116,117] treatment of Si–Cl terminated

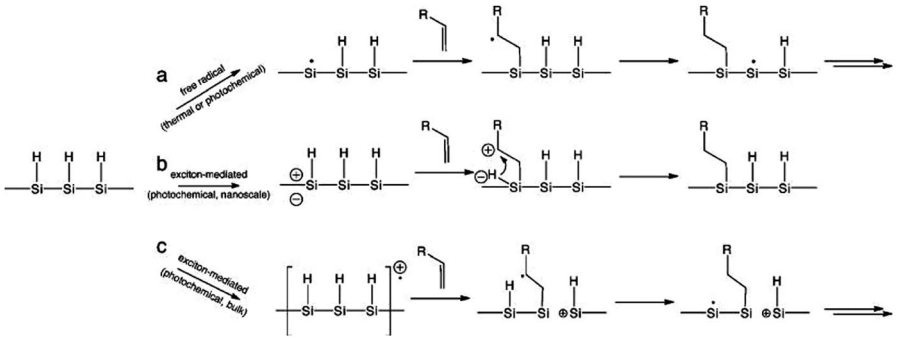

Fig. 7 Proposed mechanism of hydrosilylation on silicon nanocrystals as a free radical (a) or exciton (b) initiated processes, in comparison with exciton mediated hydrosilylation on bulk silicon (c). Reprinted with permission from Kelly *et al.*,[173] Copyright 2011 American Chemical Society.

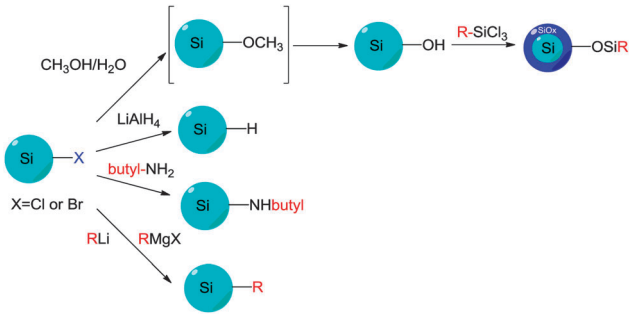

Fig. 8 Modification of chloride-terminated silicon nanocrystals. The electrophilic reactivity and versatility of the Si–X moieties are used to introduce various surface groups.

particles with $LiAlH_4$ or butyl-amine produced Si–H and Si–NH-butyl terminated particles, respectively.[80,106,170,178] Furthermore, the methoxy functionalized particles were subjects for further modifications, in a serendipitous discovery by Kauzlarich *et al.*, hydrolysis of surface Si–Cl occurred with methanol/water washing,[120] and dots were further functionalized with alkyl-trichlorosilanes, generating particles with siloxane-alkyl surfaces (Fig. 8).[120] Noticeably, silicon nanoparticles with siloxane cross-linked surface exhibit much higher stability of blue fluorescence for up to several months, in a sharp contrast to particles terminated with chloride or alkoxy surface that only lasted for two weeks.[120]

4.1.3 Advantages and drawbacks. The wet-chemical approach of surface modification to colloidal silicon nanocrystals has shown notable advantages: its compatibility with conventional bench-top chemistry allowed relatively simple experimental set-ups; most procedures are performed in solution, which is fundamentally important for applications such as ink printing and fluorescent labelling agents. However, such strategies suffer a few drawbacks. For instance, problems are sometimes encountered with complications of the air-sensitive techniques, which usually require the use of a Schlenk line or glove box. Another downside is the low boiling point of many small organic molecules that may be employed for the modification reaction, which often leads to reduction of reaction temperature to minimize evaporation. The resultant lower temperature extends reaction time, which can be for tens of hours before the final products are ready for collection. Furthermore, a minor disadvantage is the occasional agglomeration of the functionalized silicon nanocrystals in solvents, seen as a cloudy suspension from a macroscopic point of view. This phenomenon is primarily caused by the non-equilibrium competition between the attractive van der Waals forces and the interactions of the organic surface groups that stabilize particles in solution.

4.2 Surface passivation by plasma-surface interactions

In view of the above mentioned issues, and to explore new routes of surface modification for colloidal silicon nanocrystals, plasma assisted passivation has emerged as an alternative route to the wet-chemical approach. Based on the state of the plasma environment used, here we classify these methods into either aerosol, or liquid-phase plasma methods, respectively.

4.2.1 Aerosol-based plasma modification. One class of plasma-aided method of grafting molecules to the surface of silicon quantum dots involves gas-phase plasma grafting. The procedure was first demonstrated by Liao and Roberts,[179] who showed assembly of alkene, alkyne, amine and aldehyde molecules on to aerosolized silicon nanocrystals.[179] The method was recently further developed by Kortshagen *et al.*[34,39,134,141,144,169] Typically, an aerosol-based functionalization procedure requires a two part system. The first part is a synthesis component with the principle described in Section 3.3.3 (Fig. 9). In the second part, silicon nanocrystals with no surface groups were transferred by an argon gas stream into a chamber reactor, into which a vapour mixture containing desired organic molecules and argon gas was injected.[141] Vapor pressure and flow rate could be controlled by changing the bubbler equipped on the flow tap. Due to the continuous flow of the gas mixture, silicon nanocrystals were eventually collected on the filter as an orange and fluffy powder film.[141] The obtained particles were surface-functionalized, showing organic surface moieties which were confirmed by related FT-IR features, which were similar to liquid-phase modifications.[141]

4.2.2 Plasma functionalization in the liquid phase. In addition to the aerosol-based functionalization, coupling plasma with silicon nanocrystals in the liquid phase has been shown to modify the surface of particles with organic monolayers.[180–185] Several approaches were developed for liquid-phase plasma functionalization, including the use of pulsed laser,[186] direct current,[187]

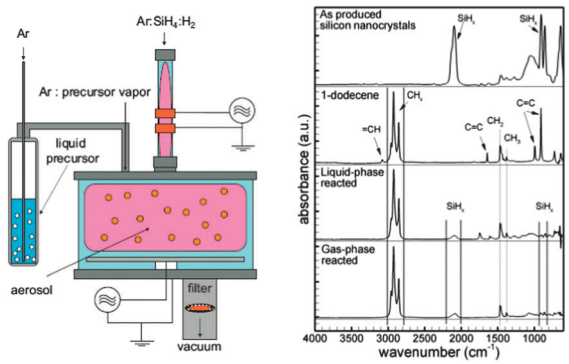

Fig. 9 Typical experimental set-up for aerosol plasma functionalization of silicon nanocrystals (left). Silicon nanocrystals functionalized by this method showed similar FT-IR features compared with liquid-phase methods. Reprinted with permission from Mangolini *et al.*[141] Copyright 2007 Wiley-VCH.

and the use of high frequency microplasma.[185] In particular, one technique utilized direct current to generate atmospheric pressure plasma between the electrode and surface of the colloidal dispersion.[187] In a typical set-up, the distance between end of the metal electrode and liquid surface was maintained between 0.5–1 mm. A counter electrode made of a carbon rod was placed ~2 cm away from the metal tube, inside which was supplied with Ar or He gas. With the application of high voltage of up to 2 kV, plasma was sustained and current was maintained between 0.5 mA and 5 mA.[187] This allowed the grafting of a number of molecules to the surface of silicon quantum dots.[187] Comparatively, microplasma was shown to be generated within a thin quartz capillary using a set of ring electrode made from copper.[188] Surface grafting of organic molecules were confirmed by FT-IR studies, which were similar to the direct-current microplasma approach.[188]

Although surface engineering on silicon nanocrystals using plasma in the liquid phase is a relatively new concept, the available data still gave some mechanistic insights into how the modification reaction occurs. It was argued that using direct current to generate the plasma may externally 'inject' electrons in the liquid phase, which induces a cascade of radical events on the particle surface, allowing the addition of organic molecules.[188] There has been no report so far showing the exact mechanism of how ultra-high frequency microplasma initiated any subsequent chemical reactions, but comparable characterization data of particle surface chemistry suggests a dominant role of plasma-electron interactions at the particle surface.[188]

4.2.3 Advantages and drawbacks. Here we reiterate the advantages and drawbacks of plasma assisted functionalization. As an alternative approach to the wet-chemical methods, one advantage of the plasma method is that the particles are negatively charged throughout the grafting process. Due to the inter-particle repulsion, the aggregation of nanocrystals clusters is minimized.[134] A second advantage is the particle confinement to the central part of the reactor. This is primarily caused by charged reactor wall that minimizes diffusion loss due to particle–wall interactions, which could significantly influence the yield of the final products.[134] A third advantage is the selective particle heating so that the actual operation temperature does not need to be very high. This is particularly true for non-thermal plasma functionalization, as the particles can be selectively heated up to hundreds of Kelvins higher compared to the surrounding gas.[39] This allowed the actual operation temperature of the equipment to be quite low, sometimes close to room temperature.[134] Last but not least, once set-up, the experiment is usually very rapid, with grafting process usually taking only a few minutes, compared to normally hours of reaction time needed for wet-chemical methods. The major disadvantage of the plasma method is the particular expertise needed to construct the entire set-up. Another issue is the non-solution environment. Both aspects are critical factors to consider for large-scale, low cost processing in applications such as ink printing and fluorescence imaging agents.

4.3 Multi-step surface modifications

There is increasing interests in further engineering of the SAM architecture after the initial modification process. Two issues are identified for single stepped surface passivations: first, when the desired surface molecules have more than one functional group, it is more favoured to use a multi-step approach than a single-step strategy, so that competition of reactions between the reactive moieties can be minimized. Second, some surface molecules are hard to synthesize and often obtained in small quantity, it is therefore easier to attach these molecules onto the first SAM, rather than directly coupling with surface silicon species. In practice, the most challenging aspect of surface passivation is often how to preserve optical properties of the particles and introduce surface functionalities at the same time. This problem can be better addressed with a multi-step process. An early example of direct modification on the first SAM layer was shown by Kauzlarich *et al.*, who demonstrated successful synthesis of siloxane coated particles *via* an intermediate hydroxyl terminated step.[120]

Recently, Shiohara *et al.* reported a reaction chain by first modifying hydrogen terminated particles with hexadiene molecule,[107] then further utilized the distal alkene group to produce epoxy, then diol functionalized particles (Fig. 10).[107] In addition, Ruizendaal *et al.* and Cheng *et al.* used thiol–ene 'click' approach of functionalization, first prepared alkene-passivated silicon quantum dots, then further reacted the terminal alkene moieties with thiol molecules with a number of distal groups (Fig. 10).[115,177] Due to the broad choices of commercially available thiols, this has allowed the production of colloidal silicon nanocrystals with a range of choice of surface functionalities.

4.4 Characterizing the surface

When characterizing the surface chemistry of colloidal silicon quantum dots, two questions are of immediate concerns. The first concern is what molecular species are actually present on the surface. It was shown that a combination of NMR, IR and XPS studies can generally give a picture of the molecular species present. The second concern is the degree of surface coverage of the SAM. It was reported that surface coverage of

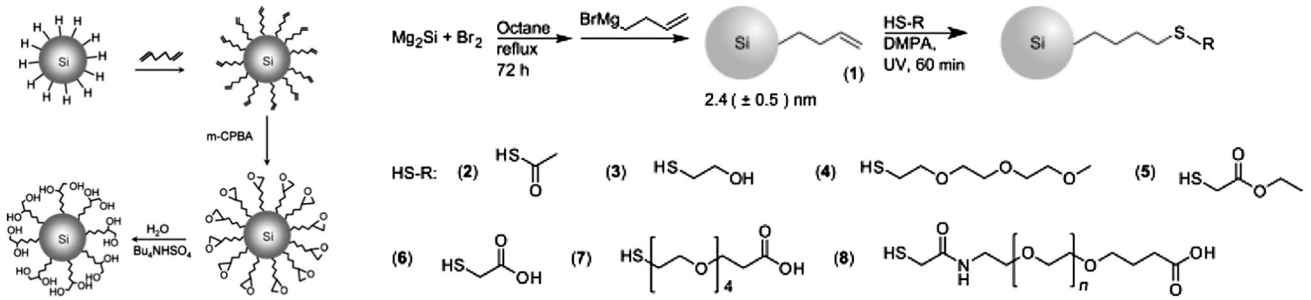

Fig. 10 Several multiple-step modification strategies. Both methods shown here rely on the preparation of alkene-functionalized particles. Reprinted with permission from Shiohara *et al.*[107] (left) and Ruizendaal *et al.*[177] (right). Copyright 2010 American Chemical Society. Copyright 2011 Wiley-VCH.

the organic monolayer was from ~55% on average to ~80% at best for flat silicon (1 0 0) and silicon (1 1 1) surface,[161] respectively. Porous silicon showed similar degree of coverage with highest reported value being 60%.[164] However, studies on the level of monolayer coverage for silicon quantum dots are still rare, though several reports are present across the literature. One study by Hua *et al.* used XPS integrated peak area to indicate approximately 50% of monolayer coverage for 1.5 nm nanocrystals in plasma assisted modification of particle surface.[132] Interestingly, the Si 2p peak measured in this work was at 102 eV, a position usually corresponding to oxides of bulk silicon, regardless both XRD and HR-TEM studies confirmed crystalline structure of the particles measured. Another study for estimating the level of surface coverage was reported by Swihart *et al.*, who used thermo-gravimetric analysis (TGA) and ^{1}H-NMR with an internal standard to show almost complete coverage of surface silicon atoms by photo-initiated hydrosilylation.[132] However, to date no single method has been widely adopted to determine surface coverage rate for silicon nanoparticles, arguably due to the difficulty in accurate size measurement and complication of the actual surface chemistry, which could be different to what was observed for flat silicon surfaces.

4.5 Impacts of surface chemistry on properties and theoretical studies

The surface chemistry for II–IV quantum dots and porous silicon has been well explored, and its importance for these nano-structured materials widely appreciated. Therefore it is unsurprising to recognize the critical role of surface chemistry for the understanding and applications of silicon nanocrystals, discussed in this section.

First, control of surface chemistry allows control over the dispersity of particles in different solvents. As many solution based methods employed dry organic solvents, products obtained often were often Si–H terminated, a moiety prone to oxidation and incompatible with hydrophilic solvents. Extra surface modifications steps are required to enable particles to be dispersible within the solvent of choice, including water. Second, due to the small size of silicon nanocrystals, and hence large proportion of surface atoms, surface states plays a pivotal role in the optoelectronic properties of silicon nanocrystals, as discussed in Section 2.2. Despite the enormous efforts dedicated to methods of preparing and surface modifying silicon nanocrystals, much fewer studies have been focused on the relationship between the optical response and surface chemistries.[42,189–192] There has been general agreement that quantum confinement, or particle size in this context, is a critical factor affecting wavelength of emission for all quantum dots. Surprisingly, silicon nanocrystals fabricated *via* etching methods usually emit in the red end of the visible spectrum,[38,167] whereas those prepared by solution reduction methods often emitted blue or green colour which appeared to be independent of particle size.[106,120,170] A recent study showed that a possible origin of the blue luminescence from silicon nanocrystals was related to the surface effect, especially due to the presence of nitrogen species on the surface.[42] Although different colours can be achieved by size separation,[76] in a joint study by the Kauzlarich, Tilley and Veinot group[42] (Fig. 11), it was shown that mixing hydrogen terminated silicon quantum dots with nitrogen containing species in the presence of oxygen induces generation of the blue peak, with increased peak height with prolonged exposure level. Last but not least, introduction of bio-active moieties allows specific binding of the particle surface with the target molecules. As an essential attribute for any fluorescence imaging agent, specific interaction of the luminescent label with biological entity of interests (*i.e.* DNA, proteins *etc.*) is of paramount

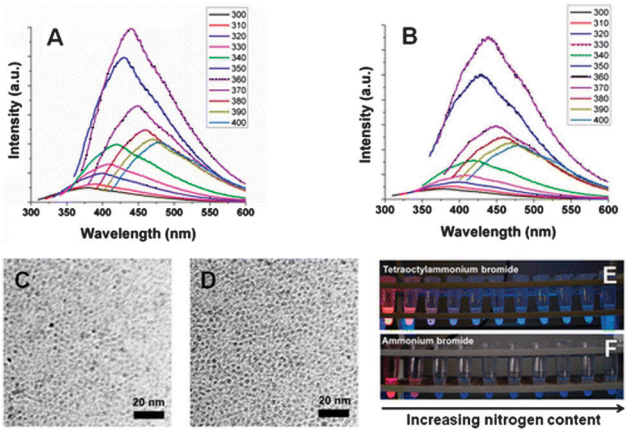

Fig. 11 Increased nitrogen species on the surface of silicon nanocrystals induces blue luminescence. Reprinted with permission from Dasog *et al.*[42] Copyright 2013 American Chemical Society.

importance for studies. More recently, it was shown that by engaging silicon with hard donor molecules, hypervalent interactions can provide both colloidal stability as well as doping SiQDs.[193]

Due to the specific techniques used for successful grafting of surface molecules, theoretical calculation has emerged as a powerful method to assist with studying the impact of surface chemistry. An early study by Brus *et al.* suggested direct band gap transitions at blue emission of H terminated, ultrasmall (<2 nm) silicon quantum dots,[194] which agreed with recent data obtained from many reduction methods.[80,106,170] According to density function theory based calculations, it was shown that the alkyl group minimally changed the optical properties of silicon quantum dots compared with Si–H particles.[195] Altering the amount of sulphur on the surface led to change of optical output.[195] In addition, a recent reported suggested that hydrosilylation increased the emission intensity, but the carbon chain length did not significantly affect the absorption and emission wavelength (Fig. 12).[189] Meanwhile, increasing surface coverage of the monolayer molecules only caused slight red-shift in the absorption spectrum, with little change in the emission profile.[189] Further calculations suggested significant decrease of both excitation and emission energy of silicon nanocrystals, but removing the carbon coating may further improve the charge carrier properties of the nanoparticles.[196] Among the various types of modifications, *ab initio* calculations suggested that introducing amine groups significantly alters emission behaviour of silicon nanocrystals for chloride coated particles,[197] which had smaller bandgap compared with hydrogen terminated particles.[198] Similarly, for fluorine passivated particles, surface effect became a more dominant factor to emission wavelength than quantum confinement for particles with size above 1.4 nm.[190] Furthermore, for oxygen bonded silicon quantum dots, it was shown that the absorption energy was not heavily affected by the surface oxygen species, but emission wavelength red-shifted due to the presence of oxygen species on the surface.[192]

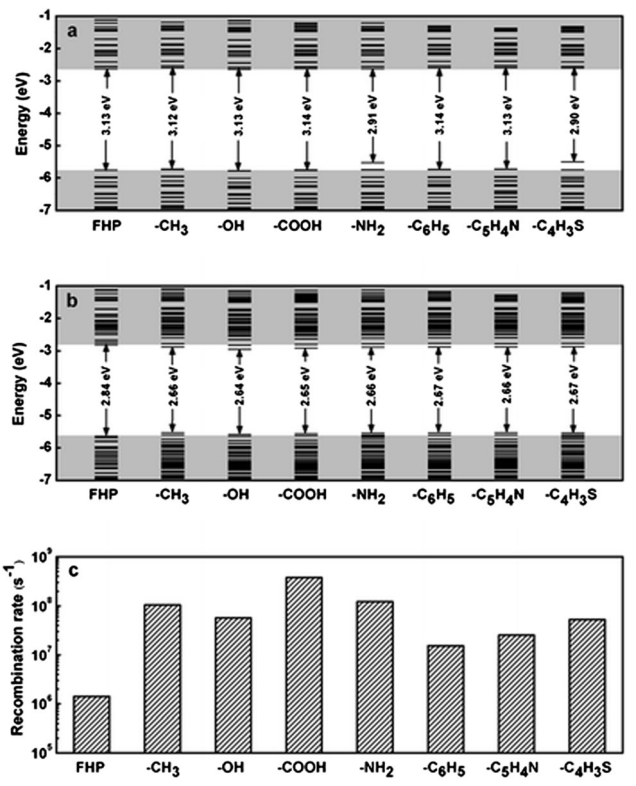

Fig. 12 Energy level diagrams of silicon quantum dots with different distal moieties at (a) ground state and (b) excited state. (c) Radiative recombination rate. FHP: full hydrogen passivation. Reprinted with permission from Wang *et al.*[189] Copyright 2012 American Chemical Society.

5. Silicon quantum dots for bio-applications

5.1 Fluorescent imaging

The potential of colloidal quantum dots in fluorescent bio-imaging applications has been well recognized. Such application is particularly relevant to quantum dots that emit in the near infrared (NIR) region of 650 nm to 900 nm, due to the existence of tissue window in which light absorption and scattering is minimized. In spite of the numerous studies of fluorescence imaging using CdSe quantum dots, the first report involving SiQDs was not published until 2004 by Li and Ruckenstein.[199] This work rapid attracted much attention, and a number of reports have been published ever since.[83,106,121,200,201]

The most typical approach for bio-imaging using SiQDs is *in vitro* studies that show the uptake of particles by cell *via* endocytosis. For instance, Alsharif *et al.* reported the intracellular internalization of alkyl-functionalized SiQDs in human neoplastic and normal primary cells.[202] It was found that cellular uptake rate was significantly faster for malignant cells in comparison with normal cells, and endocytosis was influenced by certain cholesterol derivatives.[202] Tilley *et al.* reported cellular uptake of blue-luminescent, amine coated SiQDs, with no acute cellular toxicity observed.[80,106] He *et al.* used SiQDs embedded in oxide to form nanoparticle spheres, demonstrated several endocytosis processes.[37,201] Importantly, SiQDs in these studies were not functionalized with any bio-functional moieties to target the particles to any specific locations in the cell. Hence, particles simply are located throughout the cell and therefore further modification of the particles to ensure targeted interactions are required for practical considerations.

Phospholipid-encapsulated systems have shown promise in bio-imaging applications of fluorescent nanoparticles. The advantages of using phospholipids include the good colloidal stability and low non-specific adsorption.[22] Erogbogbo *et al.* first demonstrated this process for SiQDs using hydrophobic SiQDs encapsulated in phospholipids to form micelle-type structures[83] (Fig. 13). The particle–micelle system exhibited reasonable quantum yield (2%) and biocompatibility, as demonstrated by *in vitro* imaging studies with HeLa cells.[83] A major benefit of this technique is that it offers a range of engineering choices on the micelle shell. For example, it was shown that modifying the phospholipid layer with 1,4,7,10-tetraazacyclododecane-1,4,7,10-tetraacetic acid

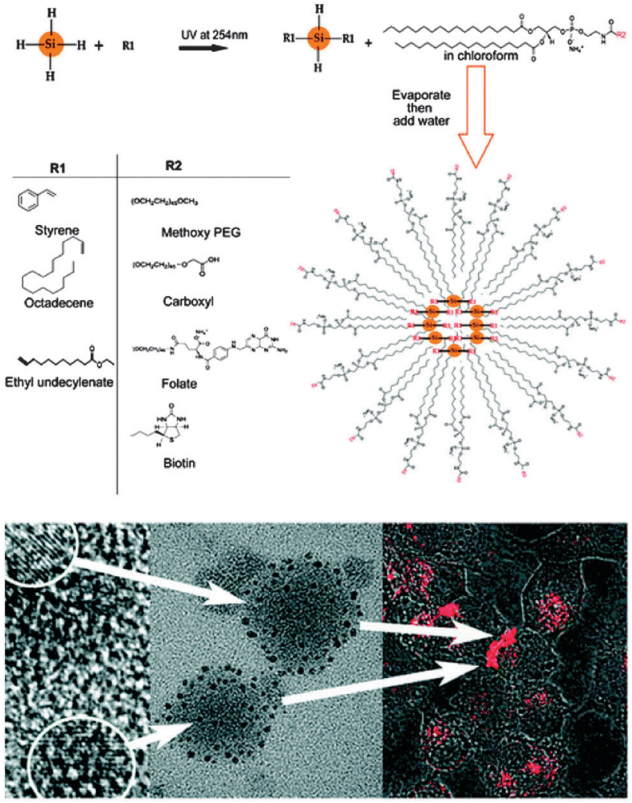

Fig. 13 SiQDs encapsulated within phospholipid micelles. TEM images suggest SiQDs contained in phospholipids are several tens of nanometers in diameters in size. Uptake of the micelle is demonstrated by fluorescence imaging of Hela cells incubated with the particles. Reprinted with permission from Erogbogbo *et al.*[83] Copyright 2008 American Chemical Society.

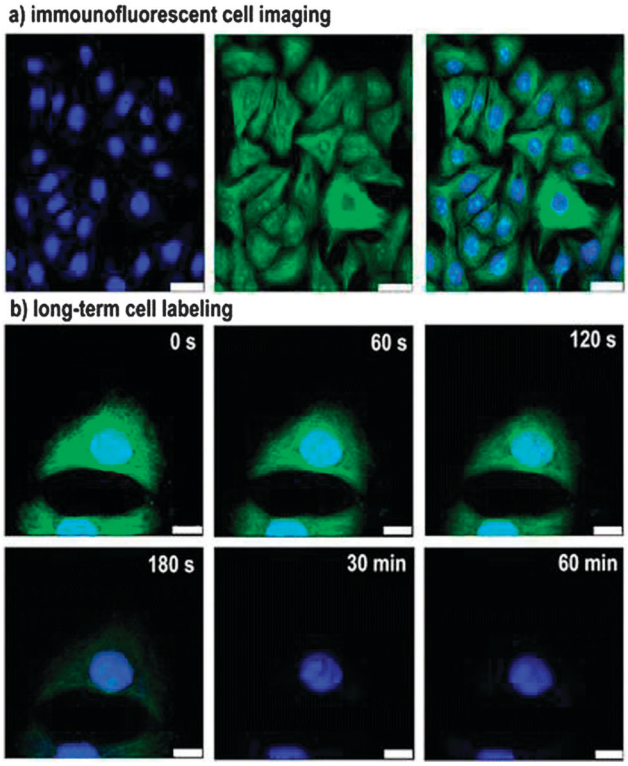

Fig. 14 Immunofluorescent cell imaging by confocal microscopy. Illustrated as staining of microtubules by FITC (Green) and nucleus by silicon nanocrystals (blue), showing no photo-bleaching of SiNCs under one hour constant illumination. Reprinted with permission from Zhong *et al.*[205] Copyright 2013 American Chemical Society.

(DOTA) ligands allowed the chelation of paramagnetic Gd ion.[203] Alternatively, coupling the micelle layer with a dye donor allowed fluorescent resonance energy transfer (FRET) to happen,[204] improving the undesired situation of fluorescence loss after encapsulation.[204]

One issue with fluorescent bio-imaging using SiQDs is the low excitation wavelength. The excitation wavelength for SiQDs is often in the UV-blue, a region that is outside of the tissue window (650–900 nm) so relevant to *in vivo* applications. One strategy to avoid the low wavelength excitation is using two photon techniques,[206] where particles are excited by two photons of half the energy.[206] It was shown that both excitation and emission can be achieved in the NIR wavelength.[207] Another issue is sometimes the large hydrodynamic diameters (>10 nm) for phospholipid-coated dots that could potentially lead to slow degradation rate.[208] Since most bio-imaging applications require the fluorescent label to be selectively attached with a biological entity, small particle radius, good colloidal stability and bio-active surfaces are equally important for bio-applicable silicon nanocrystals. It seems that these criteria can be best met with functionalization with self-assembled monolayers (SAMs).[205,209] For instance, a recent report by Zhong *et al.* showed long term cellular imaging of cell nuclei for up to 60 min with no photobleaching (Fig. 14).[205] Erogbogbo *et al.* showed selective uptake of colloidal SiQDs by cancer cells.[209] That was achieved by covalently modifying the particles *via* EDC/NHS reaction with biomolecules including lysine, folate, antimesothelin and transferrin.[209] After incubation with pancreatic cancer cells, folate and antimesothelin conjugated particles were selectively internalized by the cell.[209]

5.2 SiQDs for magnetic resonance imaging

An emerging field of using SiQDs in biomedical contexts is to explore their potential as MRI contrast agents. Although silicon by itself is not paramagnetic, paramagnetism can be achieved by adding paramagnetic species to the fluorescent dots to generate multimodalities.[203,206,210] It was shown that when co-encapsulating SiQDs with paramagnetic Fe_3O_4 nanoparticles within phospholipids, the micelle exhibited both fluorescence and paramagnetism.[210] Comparably, paramagnetism can be introduced by doping Mn directly to the particles,[206] or with attachment of a Gd-chelate on particle surface,[203] both resulted in prolonged T1 relaxation time that is desired for MRI applications. Although 'doping' is the term used here, direct evidence of alteration of the electronic structure is still lacking. The available data suggested most 'doping' attempts of SiQDs are more likely to be coordination of foreign species onto particle surface, rather than distortion of the lattice structure that was observed recently with cadmium or indium based dots.[75,211–213]

Furthermore, it was recently reported that larger silicon nanoparticles ($d \sim 350$ nm) possess ultra-long ^{29}Si magnetic hyperpolarization time which extends to tens of minutes *in vivo*.[214,215] This is remarkable as an issue for the current MR active agents is the poor signal to noise ratio, which can be greatly improved by the state of hyperpolarization of ^{29}Si *via* dynamic nuclear polarization (DNP).[214,215]

5.3 Silicon quantum dots as a less toxic alternative to conventional quantum dots

One of the more attractive aspects of SiQDs for use *in vivo* is the low intrinsic toxicity of silicon as a material. During the past-decade, advances in synthetic and surface chemistry have allowed the preparation of monodisperse, photostable quantum dots (QDs) in aqueous solutions, inspiring the design of novel fluorescent labelling agents.[20,23,148,216] However, the core materials of these quantum dots often contain heavy metal elements, such as cadmium (Cd). Due to the known toxicity of elemental Cd to biological systems, there have been intense debates over whether to use them in imaging contexts.[217,218] Although the toxicity issue of QDs has been extensively reviewed elsewhere,[27] we still highlight some of the most critical aspects here due to the importance of this topic.

Investigations into the toxicity of quantum dots began with studying *in vitro* effects. Those studies indicate that QDs associated cytotoxicity may be primarily caused by release of cadmium ions, or the generation of free radicals.[219] On the one hand, the cadmium core may contribute to biological damage caused by the QDs. One of the first systematic investigations was performed by Derfus and coworkers, who reported DNA/cell damage employing CdSe quantum dots with a variety of coating ligands.[25] In particular, it was shown that CdSe QDs release cadmium ions after UV exposure, leading to cell and DNA damage.[25] This result was supported by several other reports, suggesting the cytotoxic effects may be reduced to some extent by the coating with different surface ligands, such as mercaptoacetic acid (MAA), bovine serum albumin (BSA), mercaptoundecanoic acid (MUA), cysteamine (QD-NH_2) or thioglycerol (QD-OH), mercaptopropionic acid (MPA) and polyethylene glycol (PEG).[27,31] However, cytotoxicity cannot be completely eliminated as cell/DNA damage was observed after long term exposure to high concentration of surface coated QDs.[25,27,31] On the other hand, another series of in-depth studies showed the generation of reactive oxygen intermediates (ROI) under UV may also contribute to the QDs toxicity. Inspired by the work of Green and Howman, who demonstrated DNA nicking takes place immediately upon the addition of QDs in dark conditions,[220] electron paramagnetic resonance (EPR) studies suggested the formation of superoxide radicals from CdS dots, and hydroxyl radials from CdSe dots respectively.[221] Based on their results, Ipe *et al.* concluded that although type and amount of radicals differ from each dot, ROI is indeed produced by QDs.[221]

Concerns about the toxicity of 'conventional' QDs steered researchers towards finding cadmium-free alternatives, and in recent years a plethora of candidates have been brought to light. Indium-based QDs including InP and InP/ZnS QDs have been reported, with the latter being demonstrated for pancreatic cancer imaging.[222,223] Alternatively, $CuInS_2$–ZnS core–shell QDs have been demonstrated for sentinel lymph node imaging in both visible and near-IR region.[224–226] Zinc compounds that are often used as the shell material in conventional QDs have been put forward as a cadmium-free core material. By doping zinc-based QDs with heavy metal ions, strong emission in the visible region has been achieved.[227] ZnS:Mn/ZnS core-doped core–shell QDs were used *in vivo* for tumour imaging,[228] and recently Maity *et al.* compared the performance of three doped QD materials (Mn doped ZnS, Mn doped ZnSe and Cu doped InZnS) *in vitro*.[229]

Silicon is an attractive material for the preparation of cadmium free QDs because it is non-toxic in its bulk form and is readily degraded to silicic acid, which can be excreted in the urine.[230] Silicon has even been suggested as a trace nutrient or food additive.[231,232] Recently, a number of studies have demonstrated the low *in vitro* toxicity of SiQDs.[202,233,234] With respect to *in vivo* studies, silicon's benign nature has inspired applications in tumour vasculature targeting, sentinel lymph node mapping and multicolour imaging in mice.[208] It was shown that phospholipid encapsulated silicon quantum dots showed minimal *in vivo* toxicity at particle concentration up to $\sim$380 mg kg^{-1}, a much higher value compared with studies performed with CdSe/ZnS quantum dots.[208,235] Recently, Liu *et al.* performed *in vivo* toxicity studies of SiQDs in mice and monkeys and found no overt signs of toxicity at dose of 200 mg kg^{-1}.[133] However SiQDs did not seem to degrade as expected, although histological tests did not indicate any toxicity in monkey (Fig. 15).[133] Positron emission tomography (PET) analysis suggested that after injection, most SiQDs are rapidly excreted *via* renal filtration with the remainder accumulating in the liver for weeks with no acute toxicity observed, regardless a level of inflammation response was observed.[133,236] With all nanoparticle toxicity studies it is important to note that

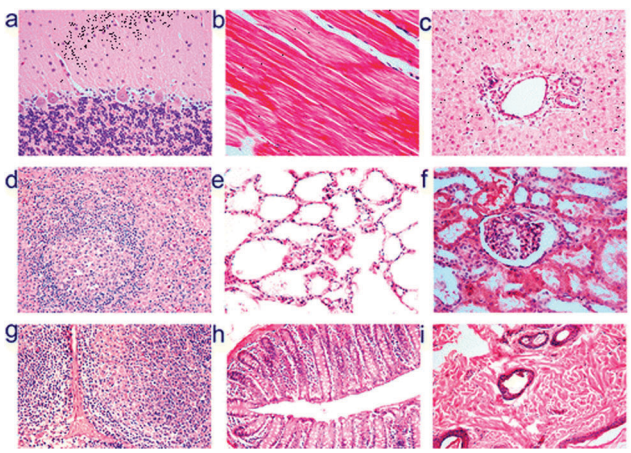

Fig. 15 Histological images of rhesus macaques indicate no toxicity of silicon nanoparticles after 3 months of injection at dose of 200 mg kg^{-1}. Images shown were tissues sample obtained from (a) brain, (b) heart, (c) liver, (d) spleen, (e) lung, (f) kidney, (g) lymph, (h) intestine and (i) skin at 40 times magnification. Reprinted with permission from Liu *et al.*[133] Copyright 2013 American Chemical Society.

capping ligands, targeting moieties, nanoparticle shape, size and surface chemistry can all elicit a cellular response.[237] For example, it was suggested that the surface chemistry of semiconductor QDs may significantly alter the potential for aggregation, and control of interface architecture have a significant impact on particle clearance from the body.[238] Hence it is vital to perform a full toxicological characterization of the nanomaterial system as it will be used in the clinic in order to elicit a full picture of the organism's response.

6. Summary and future perspectives

In this *critical review*, we aim to bring together the current most relevant knowledge on the preparation, surface modification and bio-applications of colloidal silicon nanocrystals. Even though some of the early reports on silicon quantum dots were published almost twenty years ago,[33,108] acceleration of research in this area was not seen until the new millennium. This is largely due to the slow progress in methodologies in the above mentioned sections, especially with preparation methods. The past decade has seen significant progress in these areas. As discussed in Section 3, high quality colloidal silicon quantum dots can now be prepared by a variety of routes *via* breaking down large pieces of materials or assembly of small molecular precursors. Monodisperse particles can now be prepared with good quantum yield and with reasonable control on emission, even though specific expertise is often required for such outcomes. As discussed in Section 4, the reactive particle surface is readily modifiable with well-developed, bench-top silicon chemistry, represented by the extensive use of hydrosilylation, and reactivity of halogenated particle surface. These modification techniques expanded the possibilities of utilizing colloidal silicon nanocrystals in more technology relevant contexts, such as labelling agents and sensing devices, where control of optical properties and molecular recognitions play key roles. Further motivation for the use of SiQDs *in vivo*, as an alternative to conventional metal containing QDs is given in Section 5.

Several factors to consider when working with colloidal silicon nanocrystals are: (i) Selection of preparation methods. This is particularly important when considering concentrated HF, or harsh pressure/temperature conditions were sometimes used when making the particles. Much differing to the thorough mechanistic understanding of growth kinetics of cadmium dots, there currently still lacks a feasible solution method with thorough control of size/shape and optical features for silicon quantum dots. (ii) Strategies of surface modifications. This is a mandatory step required after the initial preparation in most cases and impact of the surface states is significant to emission features. Surface modification is also essential for attaching bio-recognition moieties to the particles. Hence we predict that surface modification techniques of silicon quantum dots will draw more attentions in the future. (iii) Characterization. Although the small particle size sometimes offers convenience to simple characterization methods such as IR and solution NMR spectroscopy, characterization of the surface structures can be very problematic as modification of surface constructs progress. In practice more time can be expended on knowing what is on the surface than preparing the particles itself. It is therefore important to consolidate the tool sets of characterization. The combined toolkit of preparation, characterization and application of SiQDs is a burgeoning field which shows great promise towards the goal of routine fluorescence imaging *in vivo*.

Acknowledgements

The authors thank Australian Research Council and Australian Centre for Nanomedicine for financial support of this project.

Notes and references

1 U. Resch-Genger, M. Grabolle, S. Cavaliere-Jaricot, R. Nitschke and T. Nann, *Nat. Methods*, 2008, **5**, 763–775.
2 L. Brus, *J. Phys. Chem.*, 1986, **90**, 2555–2560.
3 L. E. Brus, *J. Chem. Phys.*, 1984, **80**, 4403–4409.
4 X. Peng, L. Manna, W. Yang, J. Wickham, E. Scher, A. Kadavanich and A. P. Alivisatos, *Nature*, 2000, **404**, 59–61.
5 A. P. Alivisatos, *J. Phys. Chem.*, 1996, **100**, 13226–13239.
6 Z. A. Peng and X. G. Peng, *J. Am. Chem. Soc.*, 2001, **123**, 183–184.
7 C. B. Murray, D. J. Norris and M. G. Bawendi, *J. Am. Chem. Soc.*, 1993, **115**, 8706–8715.
8 X. G. Peng, J. Wickham and A. P. Alivisatos, *J. Am. Chem. Soc.*, 1998, **120**, 5343–5344.
9 J. M. Garcia, G. MedeirosRibeiro, K. Schmidt, T. Ngo, J. L. Feng, A. Lorke, J. Kotthaus and P. M. Petroff, *Appl. Phys. Lett.*, 1997, **71**, 2014–2016.
10 J. Y. Marzin, J. M. Gerard, A. Izrael, D. Barrier and G. Bastard, *Phys. Rev. Lett.*, 1994, **73**, 716–719.
11 F. W. Wise, *Acc. Chem. Res.*, 2000, **33**, 773–780.
12 D. V. Talapin, A. L. Rogach, E. V. Shevchenko, A. Kornowski, M. Haase and H. Weller, *J. Am. Chem. Soc.*, 2002, **124**, 5782–5790.
13 R. J. Ellingson, M. C. Beard, J. C. Johnson, P. R. Yu, O. I. Micic, A. J. Nozik, A. Shabaev and A. L. Efros, *Nano Lett.*, 2005, **5**, 865–871.
14 I. Robel, V. Subramanian, M. Kuno and P. V. Kamat, *J. Am. Chem. Soc.*, 2006, **128**, 2385–2393.
15 P. V. Kamat, *J. Phys. Chem. C*, 2008, **112**, 18737–18753.
16 G. Conibeer, M. Green, E.-C. Cho, D. König, Y.-H. Cho, T. Fangsuwannarak, G. Scardera, E. Pink, Y. Huang, T. Puzzer, S. Huang, D. Song, C. Flynn, S. Park, X. Hao and D. Mansfield, *Thin Solid Films*, 2008, **516**, 6748–6756.
17 D. L. Huffaker, G. Park, Z. Zou, O. B. Shchekin and D. G. Deppe, *Appl. Phys. Lett.*, 1998, **73**, 2564–2566.
18 S. Strauf, K. Hennessy, M. T. Rakher, Y. S. Choi, A. Badolato, L. C. Andreani, E. L. Hu, P. M. Petroff and D. Bouwmeester, *Phys. Rev. Lett.*, 2006, **96**, 127404.
19 Q. Sun, Y. A. Wang, L. S. Li, D. Y. Wang, T. Zhu, J. Xu, C. H. Yang and Y. F. Li, *Nat. Photonics*, 2007, **1**, 717–722.

20 X. Michalet, F. F. Pinaud, L. A. Bentolila, J. M. Tsay, S. Doose, J. J. Li, G. Sundaresan, A. M. Wu, S. S. Gambhir and S. Weiss, *Science*, 2005, **307**, 538–544.
21 I. L. Medintz, H. T. Uyeda, E. R. Goldman and H. Mattoussi, *Nat. Mater.*, 2005, **4**, 435–446.
22 B. Dubertret, P. Skourides, D. J. Norris, V. Noireaux, A. H. Brivanlou and A. Libchaber, *Science*, 2002, **298**, 1759–1762.
23 M. Bruchez, M. Moronne, P. Gin, S. Weiss and A. P. Alivisatos, *Science*, 1998, **281**, 2013–2016.
24 W. C. W. Chan and S. Nie, *Science*, 1998, **281**, 2016–2018.
25 A. M. Derfus, W. C. W. Chan and S. N. Bhatia, *Nano Lett.*, 2004, **4**, 11–18.
26 N. Lewinski, V. Colvin and R. Drezek, *Small*, 2008, **4**, 26–49.
27 C. Kirchner, T. Liedl, S. Kudera, T. Pellegrino, A. M. Javier, H. E. Gaub, S. Stolzle, N. Fertig and W. J. Parak, *Nano Lett.*, 2005, **5**, 331–338.
28 G. Oberdorster, E. Oberdorster and J. Oberdorster, *Environ. Health Perspect.*, 2005, **113**, 823–839.
29 R. Hardman, *Environ. Health Perspect.*, 2006, **114**, 165–172.
30 X. H. Gao, L. L. Yang, J. A. Petros, F. F. Marshal, J. W. Simons and S. M. Nie, *Curr. Opin. Biotechnol.*, 2005, **16**, 63–72.
31 A. Hoshino, K. Fujioka, T. Oku, M. Suga, Y. F. Sasaki, T. Ohta, M. Yasuhara, K. Suzuki and K. Yamamoto, *Nano Lett.*, 2004, **4**, 2163–2169.
32 W. L. Wilson, P. F. Szajowski and L. E. Brus, *Science*, 1993, **262**, 1242–1244.
33 B. Delley and E. F. Steigmeier, *Phys. Rev. B: Condens. Matter Mater. Phys.*, 1993, **47**, 1397–1400.
34 D. Jurbergs, E. Rogojina, L. Mangolini and U. Kortshagen, *Appl. Phys. Lett.*, 2006, **88**, 233116.
35 Q. Li, Y. He, J. Chang, L. Wang, H. Chen, Y.-W. Tan, H. Wang and Z. Shao, *J. Am. Chem. Soc.*, 2013, **135**, 14924–14927.
36 J. G. Veinot, *Chem. Commun.*, 2006, 4160–4168.
37 Y. He, Z.-H. Kang, Q.-S. Li, C. H. A. Tsang, C.-H. Fan and S.-T. Lee, *Angew. Chem., Int. Ed.*, 2009, **48**, 128–132.
38 X. G. Li, Y. Q. He and M. T. Swihart, *Langmuir*, 2004, **20**, 4720–4727.
39 L. Mangolini, E. Thimsen and U. Kortshagen, *Nano Lett.*, 2005, **5**, 655–659.
40 M. R. Linford and C. E. D. Chidsey, *J. Am. Chem. Soc.*, 1993, **115**, 12631–12632.
41 M. R. Linford, P. Fenter, P. M. Eisenberger and C. E. D. Chidsey, *J. Am. Chem. Soc.*, 1995, **117**, 3145–3155.
42 M. Dasog, Z. Yang, S. Regli, T. M. Atkins, A. Faramus, M. P. Singh, E. Muthuswamy, S. M. Kauzlarich, R. D. Tilley and J. G. C. Veinot, *ACS Nano*, 2013, **7**, 2676–2685.
43 A. D. Yoffe, *Adv. Phys.*, 1993, **42**, 173–266.
44 M. Lannoo, C. Delerue, G. Allan and Y. M. Niquet, *Philos. Trans. R. Soc., A*, 2003, **361**, 259–272; discussion 272–253.
45 Y. Yin and A. P. Alivisatos, *Nature*, 2005, **437**, 664–670.
46 H. S. Mansur, *Wiley Interdiscip. Rev.: Nanomed. Nanobiotechnol.*, 2010, **2**, 113–129.
47 G. D. Scholes and G. Rumbles, *Nat. Mater.*, 2006, **5**, 683–696.
48 I. L. Medintz, H. T. Uyeda, E. R. Goldman and H. Mattoussi, *Nat. Mater.*, 2005, **4**, 435–446.
49 H. Y. Liu, M. J. Steer, T. J. Badcock, D. J. Mowbray, M. S. Skolnick, P. Navaretti, K. M. Groom, M. Hopkinson and R. A. Hogg, *Appl. Phys. Lett.*, 2005, **86**, 143108.
50 G. Allan, C. Delerue and M. Lannoo, *Phys. Rev. Lett.*, 1996, **76**, 2961–2964.
51 S. H. Tolbert, A. B. Herhold, C. S. Johnson and A. P. Alivisatos, *Phys. Rev. Lett.*, 1994, **73**, 3266–3269.
52 A. L. Efros, M. Rosen, M. Kuno, M. Nirmal, D. J. Norris and M. Bawendi, *Phys. Rev. B: Condens. Matter Mater. Phys.*, 1996, **54**, 4843–4856.
53 T. Trindade, P. O'Brien and N. L. Pickett, *Chem. Mater.*, 2001, **13**, 3843–3858.
54 A. D. Yoffe, *Adv. Phys.*, 2001, **50**, 1–208.
55 L. Landin, M. S. Miller, M. E. Pistol, C. E. Pryor and L. Samuelson, *Science*, 1998, **280**, 262–264.
56 D. Bimberg, M. Grundmann, F. Heinrichsdorff, N. N. Ledentsov, V. M. Ustinov, A. E. Zhukov, A. R. Kovsh, M. V. Maximov, Y. M. Shernyakov, B. V. Volovik, A. F. Tsatsul'nikov, P. S. Kop'ev and Z. I. Alferov, *Thin Solid Films*, 2000, **367**, 235–249.
57 R. B. Patel, A. J. Bennett, I. Farrer, C. A. Nicoll, D. A. Ritchie and A. J. Shields, *Nat. Photonics*, 2010, **4**, 632–635.
58 J. V. Frangioni, *Curr. Opin. Chem. Biol.*, 2003, **7**, 626–634.
59 W. W. Yu, L. H. Qu, W. Z. Guo and X. G. Peng, *Chem. Mater.*, 2004, **16**, 560.
60 E. Kucur, F. M. Boldt, S. Cavaliere-Jaricot, J. Ziegler and T. Nann, *Anal. Chem.*, 2007, **79**, 8987–8993.
61 D. Rueda and N. G. Walter, *Methods Mol. Biol.*, 2006, **335**, 289–310.
62 H. J. Gruber, C. D. Hahn, G. Kada, C. K. Riener, G. S. Harms, W. Ahrer, T. G. Dax and H. G. Knaus, *Bioconjugate Chem.*, 2000, **11**, 696–704.
63 S. A. Soper and Q. L. Mattingly, *J. Am. Chem. Soc.*, 1994, **116**, 3744–3752.
64 A. P. Alivisatos, W. Gu and C. Larabell, *Annu. Rev. Biomed. Eng.*, 2005, **7**, 55–76.
65 X. Y. Wang, L. H. Qu, J. Y. Zhang, X. G. Peng and M. Xiao, *Nano Lett.*, 2003, **3**, 1103–1106.
66 D. V. Talapin, I. Mekis, S. Gotzinger, A. Kornowski, O. Benson and H. Weller, *J. Phys. Chem. B*, 2004, **108**, 18826–18831.
67 L. Spanhel, M. Haase, H. Weller and A. Henglein, *J. Am. Chem. Soc.*, 1987, **109**, 5649–5655.
68 S. Xu, S. Kumar and T. Nann, *J. Am. Chem. Soc.*, 2006, **128**, 1054–1055.
69 S. H. Mihindukulasuriya, T. K. Morcone and L. B. McGown, *Electrophoresis*, 2003, **24**, 20–25.
70 M. Dahan, T. Laurence, F. Pinaud, D. S. Chemla, A. P. Alivisatos, M. Sauer and S. Weiss, *Opt. Lett.*, 2001, **26**, 825–827.
71 S. Takeoka, M. Fujii and S. Hayashi, *Phys. Rev. B: Condens. Matter Mater. Phys.*, 2000, **62**, 16820–16825.
72 X. M. Zhang, D. Neiner, S. Z. Wang, A. Y. Louie and S. M. Kauzlarich, *Nanotechnology*, 2007, **18**, 095601.

73 H. Sugimoto, M. Fujii, K. Imakita, S. Hayashi and K. Akamatsu, *J. Phys. Chem. C*, 2013, **117**, 6807–6813.
74 D. J. Norris, A. L. Efros and S. C. Erwin, *Science*, 2008, **319**, 1776–1779.
75 D. Mocatta, G. Cohen, J. Schattner, O. Millo, E. Rabani and U. Banin, *Science*, 2011, **332**, 77–81.
76 M. L. Mastronardi, F. Maier-Flaig, D. Faulkner, E. J. Henderson, C. Kübel, U. Lemmer and G. A. Ozin, *Nano Lett.*, 2011, **12**, 337–342.
77 O. Wolf, M. Dasog, Z. Yang, I. Balberg, J. G. C. Veinot and O. Millo, *Nano Lett.*, 2013, **13**, 2738–2742.
78 A. Gupta, M. T. Swihart and H. Wiggers, *Adv. Funct. Mater.*, 2009, **19**, 696–703.
79 N. Shirahata, *Phys. Chem. Chem. Phys.*, 2011, **13**, 7284–7294.
80 J. H. Warner, A. Hoshino, K. Yamamoto and R. D. Tilley, *Angew. Chem., Int. Ed.*, 2005, **44**, 4550–4554.
81 K. Dohnalova, A. N. Poddubny, A. A. Prokofiev, W. D. A. M. de Boer, C. P. Umesh, J. M. J. Paulusse, H. Zuilhof and T. Gregorkiewicz, *Light: Sci. Appl.*, 2013, **2**, e47.
82 L. Ding, T. P. Chen, Y. Liu, C. Y. Ng and S. Fung, *Phys. Rev. B: Condens. Matter Mater. Phys.*, 2005, **72**, 125419.
83 F. Erogbogbo, K. T. Yong, I. Roy, G. Xu, P. N. Prasad and M. T. Swihart, *ACS Nano*, 2008, **2**, 873–878.
84 J. A. Kelly and J. G. C. Veinot, *ACS Nano*, 2010, **4**, 4645–4656.
85 B. Bruhn, J. Valenta, F. Sangghaleh and J. Linnros, *Nano Lett.*, 2011, **11**, 5574–5580.
86 C. Galland, Y. Ghosh, A. Steinbruck, M. Sykora, J. A. Hollingsworth, V. I. Klimov and H. Htoon, *Nature*, 2011, **479**, U203–U275.
87 W. R. Cannon, S. C. Danforth, J. H. Flint, J. S. Haggerty and R. A. Marra, *J. Am. Ceram. Soc.*, 1982, **65**, 324–330.
88 O. M. Nayfeh, D. A. Antoniadis, K. Mantey and M. H. Nayfeh, *Appl. Phys. Lett.*, 2009, **94**, 043112.
89 K. Sato, H. Tsuji, K. Hirakuri, N. Fukata and Y. Yamauchi, *Chem. Commun.*, 2009, 3759–3761.
90 Z. Kang, C. H. A. Tsang, Z. Zhang, M. Zhang, N.-b. Wong, J. A. Zapien, Y. Shan and S.-T. Lee, *J. Am. Chem. Soc.*, 2007, **129**, 5326–5327.
91 Z. Kang, Y. Liu, C. H. A. Tsang, D. D. D. Ma, X. Fan, N.-B. Wong and S.-T. Lee, *Adv. Mater.*, 2009, **21**, 661–664.
92 G. Belomoin, J. Therrien, A. Smith, S. Rao, R. Twesten, S. Chaieb, M. H. Nayfeh, L. Wagner and L. Mitas, *Appl. Phys. Lett.*, 2002, **80**, 841–843.
93 M. H. Nayfeh, O. Akcakir, G. Belomoin, N. Barry, J. Therrien and E. Gratton, *Appl. Phys. Lett.*, 2000, **77**, 4086–4088.
94 M. H. Nayfeh, N. Barry, J. Therrien, O. Akcakir, E. Gratton and G. Belomoin, *Appl. Phys. Lett.*, 2001, **78**, 1131–1133.
95 C. M. Hessel, E. J. Henderson and J. G. C. Veinot, *Chem. Mater.*, 2006, **18**, 6139–6146.
96 D. Nesheva, C. Raptis, A. Perakis, I. Bineva, Z. Aneva, Z. Levi, S. Alexandrova and H. Hofmeister, *J. Appl. Phys.*, 2002, **92**, 4678–4683.
97 B. Garrido, C. Garcia, S. Y. Seo, P. Pellegrino, D. Navarro-Urrios, N. Daldosso, L. Pavesi, F. Gourbilleau and R. Rizk, *Phys. Rev. B: Condens. Matter Mater. Phys.*, 2007, **76**, 245308.
98 S.-M. Liu, Y. Yang, S. Sato and K. Kimura, *Chem. Mater.*, 2006, **18**, 637–642.
99 S.-m. Liu, S. Sato and K. Kimura, *Langmuir*, 2005, **21**, 6324–6329.
100 C. M. Hessel, M. A. Summers, A. Meldrum, M. Malac and J. G. C. Veinot, *Adv. Mater.*, 2007, **19**, 3513–3516.
101 C. M. Hessel, D. Reid, M. G. Panthani, M. R. Rasch, B. W. Goodfellow, J. Wei, H. Fujii, V. Akhavan and B. A. Korgel, *Chem. Mater.*, 2011, **24**, 393–401.
102 C. M. Hessel, E. J. Henderson and J. G. C. Veinot, *J. Phys. Chem. C*, 2007, **111**, 6956–6961.
103 J. A. Kelly, E. J. Henderson and J. G. Veinot, *Chem. Commun.*, 2010, **46**, 8704–8718.
104 F. Hua, M. T. Swihart and E. Ruckenstein, *Langmuir*, 2005, **21**, 6054–6062.
105 E. J. Henderson and J. G. C. Veinot, *Chem. Mater.*, 2007, **19**, 1886–1888.
106 R. D. Tilley and K. Yamamoto, *Adv. Mater.*, 2006, **18**, 2053–2056.
107 A. Shiohara, S. Hanada, S. Prabakar, K. Fujioka, T. H. Lim, K. Yamamoto, P. T. Northcote and R. D. Tilley, *J. Am. Chem. Soc.*, 2010, **132**, 248–253.
108 J. R. Heath, *Science*, 1992, **258**, 1131–1133.
109 R. K. Baldwin, K. A. Pettigrew, E. Ratai, M. P. Augustine and S. M. Kauzlarich, *Chem. Commun.*, 2002, 1822–1823.
110 N. Arul Dhas, C. P. Raj and A. Gedanken, *Chem. Mater.*, 1998, **10**, 3278–3281.
111 J. P. Wilcoxon, G. A. Samara and P. N. Provencio, *Phys. Rev. B: Condens. Matter Mater. Phys.*, 1999, **60**, 2704–2714.
112 S. Prabakar, A. Shiohara, S. Hanada, K. Fujioka, K. Yamamoto and R. D. Tilley, *Chem. Mater.*, 2010, **22**, 482–486.
113 A. Shiohara, S. Prabakar, A. Faramus, C. Y. Hsu, P. S. Lai, P. T. Northcote and R. D. Tilley, *Nanoscale*, 2011, **3**, 3364–3370.
114 J. Wang, S. Sun, F. Peng, L. Cao and L. Sun, *Chem. Commun.*, 2011, **47**, 4941–4943.
115 X. Y. Cheng, R. Gondosiswanto, S. Ciampi, P. J. Reece and J. J. Gooding, *Chem. Commun.*, 2012, **48**, 11874–11876.
116 C. S. Yang, R. A. Bley, S. M. Kauzlarich, H. W. H. Lee and G. R. Delgado, *J. Am. Chem. Soc.*, 1999, **121**, 5191–5195.
117 D. Mayeri, B. L. Phillips, M. P. Augustine and S. M. Kauzlarich, *Chem. Mater.*, 2001, **13**, 765–770.
118 R. K. Baldwin, K. A. Pettigrew, J. C. Garno, P. P. Power, G. Y. Liu and S. M. Kauzlarich, *J. Am. Chem. Soc.*, 2002, **124**, 1150–1151.
119 R. A. Bley and S. M. Kauzlarich, *J. Am. Chem. Soc.*, 1996, **118**, 12461–12462.
120 J. Zou, R. K. Baldwin, K. A. Pettigrew and S. M. Kauzlarich, *Nano Lett.*, 2004, **4**, 1181–1186.
121 B. A. Manhat, A. L. Brown, L. A. Black, J. B. A. Ross, K. Fichter, T. Vu, E. Richman and A. M. Goforth, *Chem. Mater.*, 2011, **23**, 2407–2418.
122 C.-S. Yang, R. A. Bley, S. M. Kauzlarich, H. W. H. Lee and G. R. Delgado, *J. Am. Chem. Soc.*, 1999, **121**, 5191–5195.
123 J. D. Holmes, K. J. Ziegler, R. C. Doty, L. E. Pell, K. P. Johnston and B. A. Korgel, *J. Am. Chem. Soc.*, 2001, **123**, 3743–3748.

124 D. S. English, L. E. Pell, Z. H. Yu, P. F. Barbara and B. A. Korgel, *Nano Lett.*, 2002, **2**, 681–685.
125 Y. He, Y. L. Zhong, F. Peng, X. P. Wei, Y. Y. Su, Y. M. Lu, S. Su, W. Gu, L. S. Liao and S. T. Lee, *J. Am. Chem. Soc.*, 2011, **133**, 14192–14195.
126 W. R. Cannon, S. C. Danforth, J. S. Haggerty and R. A. Marra, *J. Am. Ceram. Soc.*, 1982, **65**, 330–335.
127 F. Huisken, B. Kohn and V. Paillard, *Appl. Phys. Lett.*, 1999, **74**, 3776–3778.
128 G. Ledoux, J. Gong and F. Huisken, *Appl. Phys. Lett.*, 2001, **79**, 4028–4030.
129 G. Ledoux, J. Gong, F. Huisken, O. Guillois and C. Reynaud, *Appl. Phys. Lett.*, 2002, **80**, 4834–4836.
130 K. Potrick, T. Schmidt, S. Bublitz, C. Muhlig, W. Paa and F. Huisken, *Appl. Phys. Lett.*, 2011, **98**, 083111.
131 L. B. Ma, T. Schmidt, O. Guillois and F. Huisken, *Appl. Phys. Lett.*, 2009, **95**, 013115.
132 F. J. Hua, M. T. Swihart and E. Ruckenstein, *Langmuir*, 2005, **21**, 6054–6062.
133 J. Liu, F. Erogbogbo, K.-T. Yong, L. Ye, J. Liu, R. Hu, H. Chen, Y. Hu, Y. Yang, J. Yang, I. Roy, N. A. Karker, M. T. Swihart and P. N. Prasad, *ACS Nano*, 2013, **7**, 7303–7310.
134 U. Kortshagen, *J. Phys. D: Appl. Phys.*, 2009, **42**, 113001.
135 G. Viera, S. Huet, M. Mikikian and L. Boufendi, *Thin Solid Films*, 2002, **403**, 467–470.
136 G. Viera, M. Mikikian, E. Bertran, P. R. I. Cabarrocas and L. Boufendi, *J. Appl. Phys.*, 2002, **92**, 4684–4694.
137 M. Otobe, T. Kanai, T. Ifuku, H. Yajima and S. Oda, *J. Non-Cryst. Solids*, 1996, **198**, 875–878.
138 S. Oda, *Adv. Colloid Interface Sci.*, 1997, **71–72**, 31–47.
139 S. Oda and M. Otobe, in *Microcrystalline and Nanocrystalline Semiconductors*, ed. R. W. Collins, C. C. Tsai, M. Hirose, F. Koch and L. Brus, Materials Research Soc., Pittsburgh, 1995, vol. 358, pp. 721–731.
140 A. Bapat, M. Gatti, Y.-P. Ding, S. A. Campbell and U. Kortshagen, *J. Phys. D: Appl. Phys.*, 2007, **40**, 2247–2257.
141 L. Mangolini and U. Kortshagen, *Adv. Mater.*, 2007, **19**, 2513–2519.
142 L. Mangolini, E. Thimsen and U. Kortshagen, in *Amorphous and Nanocrystalline Silicon Science and Technology-2005*, ed. R. W. Collins, P. C. Taylor, M. Kondo, R. Carius and R. Biswas, 2005, vol. 862, pp. 307–312.
143 L. Mangolini, D. Jurbergs, E. Rogojina and U. Kortshagen, *J. Lumin.*, 2006, **121**, 327–334.
144 U. Kortshagen, L. Mangolini and A. Bapat, *J. Nanopart. Res.*, 2007, **9**, 39–52.
145 X. D. Pi, L. Mangolini, S. A. Campbell and U. Kortshagen, *Phys. Rev. B: Condens. Matter Mater. Phys.*, 2007, **75**, 085423.
146 J. Knipping, H. Wiggers, B. Rellinghaus, P. Roth, D. Konjhodzic and C. Meier, *J. Nanosci. Nanotechnol.*, 2004, **4**, 1039–1044.
147 R. M. Sankaran, D. Holunga, R. C. Flagan and K. P. Giapis, *Nano Lett.*, 2005, **5**, 537–541.
148 I. L. Medintz, H. T. Uyeda, E. R. Goldman and H. Mattoussi, *Nat. Mater.*, 2005, **4**, 435–446.
149 D. Gerion, F. Pinaud, S. C. Williams, W. J. Parak, D. Zanchet, S. Weiss and A. P. Alivisatos, *J. Phys. Chem. B*, 2001, **105**, 8861–8871.
150 A. Burns, H. Ow and U. Wiesner, *Chem. Soc. Rev.*, 2006, **35**, 1028–1042.
151 P. Mulvaney, L. M. Liz-Marzan, M. Giersig and T. Ung, *J. Mater. Chem.*, 2000, **10**, 1259–1270.
152 F. Dubois, B. Mahler, B. Dubertret, E. Doris and C. Mioskowski, *J. Am. Chem. Soc.*, 2007, **129**, 482–483.
153 S. F. Wuister, C. D. Donega and A. Meijerink, *J. Phys. Chem. B*, 2004, **108**, 17393–17397.
154 N. Gaponik, D. V. Talapin, A. L. Rogach, K. Hoppe, E. V. Shevchenko, A. Kornowski, A. Eychmuller and H. Weller, *J. Phys. Chem. B*, 2002, **106**, 7177–7185.
155 A. Shavel, N. Gaponik and A. Eychmuller, *J. Phys. Chem. B*, 2006, **110**, 19280–19284.
156 A. Eychmuller and A. L. Rogach, *Pure Appl. Chem.*, 2000, **72**, 179–188.
157 C.-A. J. Lin, R. A. Sperling, J. K. Li, T.-Y. Yang, P.-Y. Li, M. Zanella, W. H. Chang and W. J. Parak, *Small*, 2008, **4**, 334–341.
158 N. Tomczak, D. Janczewski, M. Y. Han and G. J. Vancso, *Prog. Polym. Sci.*, 2009, **34**, 393–430.
159 W. W. Yu, E. Chang, J. C. Falkner, J. Y. Zhang, A. M. Al-Somali, C. M. Sayes, J. Johns, R. Drezek and V. L. Colvin, *J. Am. Chem. Soc.*, 2007, **129**, 2871–2879.
160 J. Tang, K. W. Kemp, S. Hoogland, K. S. Jeong, H. Liu, L. Levina, M. Furukawa, X. H. Wang, R. Debnath, D. K. Cha, K. W. Chou, A. Fischer, A. Amassian, J. B. Asbury and E. H. Sargent, *Nat. Mater.*, 2011, **10**, 765–771.
161 S. Ciampi, J. B. Harper and J. J. Gooding, *Chem. Soc. Rev.*, 2010, **39**, 2158–2183.
162 N. S. Bhairamadgi, S. Gangarapu, M. A. C. Campos, J. M. J. Paulusse, C. J. M. van Rijn and H. Zuilhof, *Langmuir*, 2013, **29**, 4535–4542.
163 S. Ciampi, T. Bocking, K. A. Kilian, M. James, J. B. Harper and J. J. Gooding, *Langmuir*, 2007, **23**, 9320–9329.
164 T. Bocking, K. A. Kilian, K. Gaus and J. J. Gooding, *Adv. Funct. Mater.*, 2008, **18**, 3827–3833.
165 E. J. Anglin, L. Y. Cheng, W. R. Freeman and M. J. Sailor, *Adv. Drug Delivery Rev.*, 2008, **60**, 1266–1277.
166 K. A. Kilian, T. Bocking, K. Gaus, M. Gal and J. J. Gooding, *Biomaterials*, 2007, **28**, 3055–3062.
167 J. R. Rodríguez Núñez, J. A. Kelly, E. J. Henderson and J. G. C. Veinot, *Chem. Mater.*, 2011, **24**, 346–352.
168 Z. H. Kang, C. H. A. Tsang, N. B. Wong, Z. D. Zhang and S. T. Lee, *J. Am. Chem. Soc.*, 2007, **129**, 12090–12091.
169 L. Mangolini, E. Thimsen and U. Kortshagen, *Amorphous and Nanocrystalline Silicon Science and Technology-2005*, 2005, vol. 862, pp. 307–312.
170 R. D. Tilley, J. H. Warner, K. Yamamoto, I. Matsui and H. Fujimori, *Chem. Commun.*, 2005, 1833–1835.
171 X. Li and P. W. Bohn, *Appl. Phys. Lett.*, 2000, **77**, 2572–2574.
172 C. M. Hessel, E. J. Henderson, J. A. Kelly, R. G. Cavell, T.-K. Sham and J. G. C. Veinot, *J. Phys. Chem. C*, 2008, **112**, 14247–14254.

173 J. A. Kelly, A. M. Shukaliak, M. D. Fleischauer and J. G. C. Veinot, *J. Am. Chem. Soc.*, 2011, **133**, 9564–9571.
174 Y. Yu, C. M. Hessel, T. D. Bogart, M. G. Panthani, M. R. Rasch and B. A. Korgel, *Langmuir*, 2013, **29**, 1533–1540.
175 M. Rosso-Vasic, E. Spruijt, Z. Popovic, K. Overgaag, B. van Lagen, B. Grandidier, D. Vanmaekelbergh, D. Dominguez-Gutierrez, L. De Cola and H. Zuilhof, *J. Mater. Chem.*, 2009, **19**, 5926–5933.
176 J. R. Siekierzycka, M. Rosso-Vasic, H. Zuilhof and A. M. Brouwer, *J. Phys. Chem. C*, 2011, **115**, 20888–20895.
177 L. Ruizendaal, S. P. Pujari, V. Gevaerts, J. M. Paulusse and H. Zuilhof, *Chem.–Asian J.*, 2011, **6**, 2776–2786.
178 E. Rogozhina, G. Belomoin, A. Smith, L. Abuhassan, N. Barry, O. Akcakir, P. V. Braun and M. H. Nayfeh, *Appl. Phys. Lett.*, 2001, **78**, 3711–3713.
179 Y.-C. Liao and J. T. Roberts, *J. Am. Chem. Soc.*, 2006, **128**, 9061–9065.
180 V. Svrcek, D. Mariotti and M. Kondo, *Appl. Phys. Lett.*, 2010, **97**, 161502.
181 V. Svrcek, T. Yamanari, D. Mariotti, K. Matsubara and M. Kondo, *Appl. Phys. Lett.*, 2012, **100**, 223904.
182 J. McKenna, J. Patel, S. Mitra, N. Soin, V. Svrcek, P. Maguire and D. Mariotti, *Eur. Phys. J.: Appl. Phys.*, 2011, **56**, 24020.
183 D. Mariotti and R. M. Sankaran, *J. Phys. D: Appl. Phys.*, 2010, **43**, 323001.
184 D. Mariotti and R. M. Sankaran, *J. Phys. D: Appl. Phys.*, 2011, **44**, 174023.
185 D. Mariotti, J. Patel, V. Svrcek and P. Maguire, *Plasma Processes Polym.*, 2012, **9**, 1074–1085.
186 V. Svrcek, D. Mariotti, Y. Shibata and M. Kondo, *J. Phys. D: Appl. Phys.*, 2010, **43**, 415402.
187 D. Mariotti, V. Svrcek, J. W. J. Hamilton, M. Schmidt and M. Kondo, *Adv. Funct. Mater.*, 2012, **22**, 954–964.
188 D. Mariotti, S. Mitra and V. Svrcek, *Nanoscale*, 2013, **5**, 1385–1398.
189 R. Wang, X. D. Pi and D. R. Yang, *J. Phys. Chem. C*, 2012, **116**, 19434–19443.
190 Y. Ma, X. Pi and D. Yang, *J. Phys. Chem. C*, 2012, **116**, 5401–5406.
191 M. J. Llansola Portolés, R. Pis Diez, M. L. Dell'Arciprete, P. Caregnato, J. J. Romero, D. O. Mártire, O. Azzaroni, M. Ceolín and M. C. Gonzalez, *J. Phys. Chem. C*, 2012, **116**, 11315–11325.
192 X. Chen, X. Pi and D. Yang, *J. Phys. Chem. C*, 2010, **114**, 8774–8781.
193 L. M. Wheeler, N. R. Neale, T. Chen and U. R. Kortshagen, *Nat. Commun.*, 2013, **4**, 2197.
194 Z. Y. Zhou, L. Brus and R. Friesner, *Nano Lett.*, 2003, **3**, 163–167.
195 Q. S. Li, R. Q. Zhang, S. T. Lee, T. A. Niehaus and T. Frauenheim, *J. Chem. Phys.*, 2008, **128**, 244714.
196 Z. Y. Ni, X. D. Pi and D. R. Yang, *RSC Adv.*, 2012, **2**, 11227–11230.
197 R. Wang, X. Pi and D. Yang, *Phys. Chem. Chem. Phys.*, 2013, **15**, 1815–1820.
198 A. Carvalho, S. Oberg, M. J. Rayson and P. R. Briddon, *J. Nanosci. Nanotechnol.*, 2013, **13**, 1039–1042.
199 Z. F. Li and E. Ruckenstein, *Nano Lett.*, 2004, **4**, 1463–1467.
200 E. J. Henderson, A. J. Shuhendler, P. Prasad, V. Baumann, F. Maier-Flaig, D. O. Faulkner, U. Lemmer, X. Y. Wu and G. A. Ozin, *Small*, 2011, **7**, 2507–2516.
201 Y. He, Y. Su, X. Yang, Z. Kang, T. Xu, R. Zhang, C. Fan and S.-T. Lee, *J. Am. Chem. Soc.*, 2009, **131**, 4434–4438.
202 N. H. Alsharif, C. E. M. Berger, S. S. Varanasi, Y. Chao, B. R. Horrocks and H. K. Datta, *Small*, 2009, **5**, 221–228.
203 F. Erogbogbo, C. W. Chang, J. L. May, L. Liu, R. Kumar, W. C. Law, H. Ding, K. T. Yong, I. Roy, M. Sheshadri, M. T. Swihart and P. N. Prasad, *Nanoscale*, 2012, **4**, 5483–5489.
204 F. Erogbogbo, C. W. Chang, J. May, P. N. Prasad and M. T. Swihart, *Nanoscale*, 2012, **4**, 5163–5168.
205 Y. Zhong, F. Peng, F. Bao, S. Wang, X. Ji, L. Yang, Y. Su, S.-T. Lee and Y. He, *J. Am. Chem. Soc.*, 2013, **135**, 8350–8356.
206 C. Q. Tu, X. C. Ma, P. Pantazis, S. M. Kauzlarich and A. Y. Louie, *J. Am. Chem. Soc.*, 2010, **132**, 2016–2023.
207 J. Liu, F. Erogbogbo, K.-T. Yong, L. Ye, J. Liu, R. Hu, H. Chen, Y. Hu, Y. Yang, J. Yang, I. Roy, N. A. Karker, M. T. Swihart and P. N. Prasad, *ACS Nano*, 2013, **7**, 7303–7310.
208 F. Erogbogbo, K. T. Yong, I. Roy, R. Hu, W. C. Law, W. Zhao, H. Ding, F. Wu, R. Kumar, M. T. Swihart and P. N. Prasad, *ACS Nano*, 2011, **5**, 413–423.
209 F. Erogbogbo, C. A. Tien, C. W. Chang, K. T. Yong, W. C. Law, H. Ding, I. Roy, M. T. Swihart and P. N. Prasad, *Bioconjugate Chem.*, 2011, **22**, 1081–1088.
210 F. Erogbogbo, K. T. Yong, R. Hu, W. C. Law, H. Ding, C. W. Chang, P. N. Prasad and M. T. Swihart, *ACS Nano*, 2010, **4**, 5131–5138.
211 V. C. Holmberg, J. R. Helps, K. A. Mkhoyan and D. J. Norris, *Chem. Mater.*, 2013, **25**, 1332–1350.
212 A. A. Gunawan, K. A. Mkhoyan, A. W. Wills, M. G. Thomas and D. J. Norris, *Nano Lett.*, 2011, **11**, 5553–5557.
213 A. Sahu, M. S. Kang, A. Kompch, C. Notthoff, A. W. Wills, D. Deng, M. Winterer, C. D. Frisbie and D. J. Norris, *Nano Lett.*, 2012, **12**, 2587–2594.
214 J. W. Aptekar, M. C. Cassidy, A. C. Johnson, R. A. Barton, M. Lee, A. C. Ogier, C. Vo, M. N. Anahtar, Y. Ren, S. N. Bhatia, C. Ramanathan, D. G. Cory, A. L. Hill, R. W. Mair, M. S. Rosen, R. L. Walsworth and C. M. Marcus, *ACS Nano*, 2009, **3**, 4003–4008.
215 M. C. Cassidy, H. R. Chan, B. D. Ross, P. K. Bhattacharya and C. M. Marcus, *Nat. Nanotechnol.*, 2013, **8**, 363–368.
216 A. M. Smith, H. Duan, A. M. Mohs and S. Nie, *Adv. Drug Delivery Rev.*, 2008, **60**, 1226–1240.
217 R. Hardman, *Environ. Health Perspect.*, 2006, **114**, 165–172.
218 T. S. Hauck, R. E. Anderson, H. C. Fischer, S. Newbigging and W. C. Chan, *Small*, 2010, **6**, 138–144.
219 M. Bottrill and M. Green, *Chem. Commun.*, 2011, **47**, 7039–7050.
220 M. Green and E. Howman, *Chem. Commun.*, 2005, 121–123.
221 B. I. Ipe, M. Lehnig and C. M. Niemeyer, *Small*, 2005, **1**, 706–709.

222 D. J. Bharali, D. W. Lucey, H. Jayakumar, H. E. Pudavar and P. N. Prasad, *J. Am. Chem. Soc.*, 2005, **127**, 11364–11371.
223 K.-T. Yong, H. Ding, I. Roy, W.-C. Law, E. J. Bergey, A. Maitra and P. N. Prasad, *ACS Nano*, 2009, **3**, 502–510.
224 L. Li, T. J. Daou, I. Texier, T. T. Kim Chi, N. Q. Liem and P. Reiss, *Chem. Mater.*, 2009, **21**, 2422–2429.
225 T. Pons, E. Pic, N. Lequeux, E. Cassette, L. Bezdetnaya, F. Guillemin, F. Marchal and B. Dubertret, *ACS Nano*, 2010, **4**, 2531–2538.
226 M. Helle, E. Cassette, L. Bezdetnaya, T. Pons, A. Leroux, F. Plénat, F. Guillemin, B. Dubertret and F. Marchal, *PLoS One*, 2012, **7**, e44433.
227 N. Pradhan, D. Goorskey, J. Thessing and X. G. Peng, *J. Am. Chem. Soc.*, 2005, **127**, 17586–17587.
228 Z. Yu, X. Ma, B. Yu, Y. Pan and Z. Liu, *J. Biomater. Appl.*, 2013, **28**, 232–240.
229 A. R. Maity, S. Palmal, S. K. Basiruddin, N. S. Karan, S. Sarkar, N. Pradhan and N. R. Jana, *Nanoscale*, 2013, **5**, 5506–5513.
230 K. Fujioka, M. Hiruoka, K. Sato, N. Manabe, R. Miyasaka, S. Hanada, A. Hoshino, R. D. Tilley, Y. Manome, K. Hirakuri and K. Yamamoto, *Nanotechnology*, 2008, **19**, 415102.
231 S. Sripanyakorn, R. Jugdaohsingh, R. P. H. Thompson and J. J. Powell, *Nutr. Bull.*, 2005, **30**, 222–230.
232 L. T. Canham, *Nanotechnology*, 2007, **18**, 185704.
233 J. Choi, Q. Zhang, V. Reipa, N. S. Wang, M. E. Stratmeyer, V. M. Hitchins and P. L. Goering, *J. Appl. Toxicol.*, 2009, **29**, 52–60.
234 Q. Wang, Y. Bao, X. Zhang, P. R. Coxon, U. A. Jayasooriya and Y. Chao, *Adv. Healthcare Mater.*, 2012, **1**, 189–198.
235 X. Gao, Y. Cui, R. M. Levenson, L. W. K. Chung and S. Nie, *Nat. Biotechnol.*, 2004, **22**, 969–976.
236 C. Tu, X. Ma, A. House, S. M. Kauzlarich and A. Y. Louie, *ACS Med. Chem. Lett.*, 2011, **2**, 285–288.
237 A. Nel, T. Xia, L. Mädler and N. Li, *Science*, 2006, **311**, 622–627.
238 H. C. Fischer, L. C. Liu, K. S. Pang and W. C. W. Chan, *Adv. Funct. Mater.*, 2006, **16**, 1299–1305.
239 J. L. Heinrich, C. L. Curtis, G. M. Credo, M. J. Sailor and K. L. Kavanagh, *Science*, 1992, **255**, 66–68.

